*J Physiol* 599.23 (2021) pp 5281–5300



The Journal of Physiology

# Hydrogen peroxide and phosphoinositide metabolites synergistically regulate a cation current to influence neuroendocrine cell bursting

Alamjeet K. Chauhan-Puri, Kelly H. Lee and Neil S. Magoski

*Department of Biomedical and Molecular Sciences, Experimental Medicine Graduate Program, Queen's University, Kingston, Ontario, Canada*

Edited by: Katalin Toth & Jean-Claude Béïque

The peer review history is available in the Supporting Information section of this article (https://doi.org/10.1113/JP282302#support-information-section).

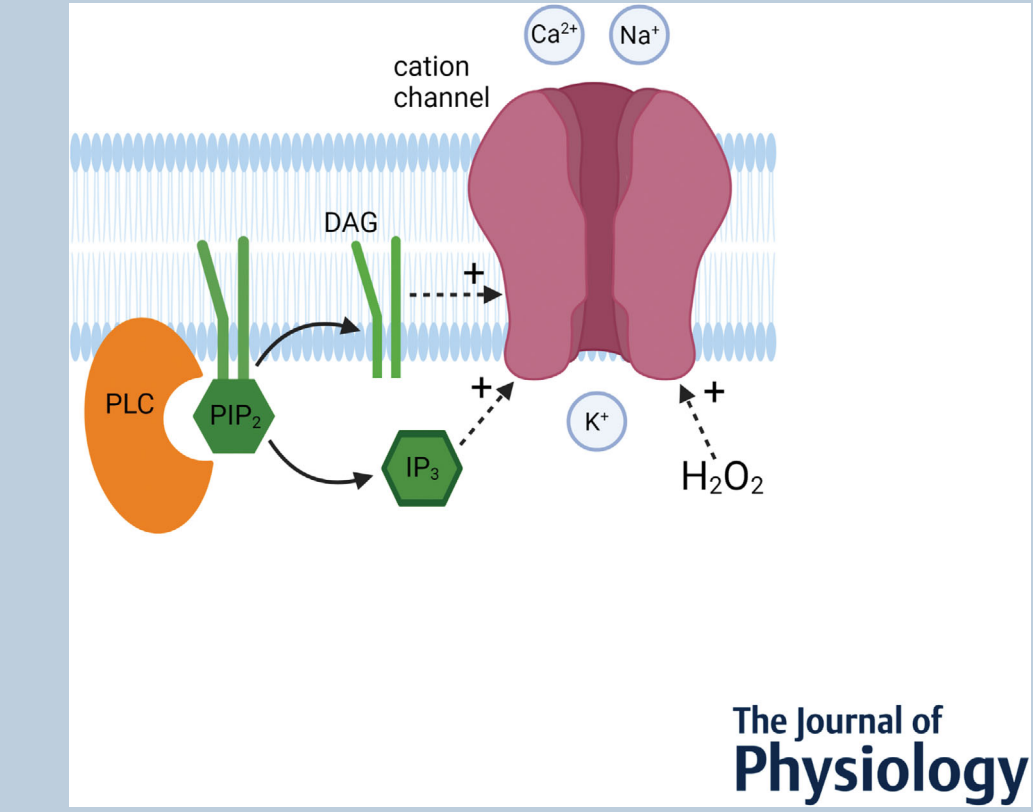


**Abstract** In various neurons, including neuroendocrine cells, non-selective cation channels elicit plateau potentials and persistent firing. Reproduction in the marine snail *Aplysia californica* is initiated when the neuroendocrine bag cell neurons undergo an afterdischarge,

**Alamjeet Chauhan-Puri** completed her PhD in Experimental Medicine at Queen's University on ion channels and reactive oxygen species. H2O2 is a reactive oxygen species by-product of metabolism, and linked to inflammation, cell death, ageing, and neurodegeneration. However, she found a role for $H_2O_2$ in normal physiology using the marine snail *Aplysia californica*. Specifically, $H_2O_2$ opens a non-selective cationic conductance in neuroendocrine cells, which causes a prolonged afterdischarge and hormone release, leading to reproductive behaviour. She now shows that phosphoinositide metabolites enhance the $H_2O_2$-gated channel to further promote bursting. Her work is consistent with reactive oxygen species also acting as neuromodulators.



DOI: 10.1113/JP282302

that is, a prolonged period of enhanced excitability and spiking during which egg-laying hormone is released into the blood. The afterdischarge is associated with both the production of hydrogen peroxide ($H_2O_2$) and activation of phospholipase C (PLC), which hydrolyses phosphatidylinositol-4,5-bisphosphate into diacylglycerol (DAG) and inositol trisphosphate ($IP_3$). We previously demonstrated that $H_2O_2$ gates a voltage-dependent cation current and evokes spiking in bag cell neurons. The present study tests if DAG and $IP_3$ impact the $H_2O_2$-induced current and excitability. In whole-cell voltage-clamped cultured bag cell neurons, bath-application of 1-oleoyl-2-acetyl-*sn*-glycerol (OAG), a DAG analogue, enhanced the $H_2O_2$-induced current, which was amplified by the inclusion of $IP_3$ in the pipette. A similar outcome was produced by the PLC activator, *N*-(3-trifluoromethylphenyl)-2,4,6-trimethylbenzenesul fonamide. In current-clamp, OAG or OAG plus $IP_3$, elevated the frequency of $H_2O_2$-induced bursting. PKC is also triggered during the afterdischarge; when PKC was stimulated with phorbol 12-myristate 13-acetate, it caused a voltage-dependent inward current with a reversal potential similar to the $H_2O_2$-induced current. Furthermore, PKC activation followed by $H_2O_2$ reduced the onset latency and increased the duration of action potential firing. Finally, inhibiting nicotinamide adenine dinucleotide phosphate oxidase with 3-benzyl-7-(2-benzoxazolyl)thio-1,2,3-triazolo[4,5-d]pyrimidine diminished evoked bursting in isolated bag cell neuron clusters. These results suggest that reactive oxygen species and phosphoinostide metabolites may synergize and contribute to reproductive behaviour by promoting neuroendocrine cell firing.

(Received 27 August 2021; accepted after revision 7 October 2021; first published online 22 October 2021)
**Corresponding author** N. S. Magoski: Department of Biomedical and Molecular Sciences, Experimental Medicine Graduate Program, Queen's University, Botterell Hall, 18 Stuart Street, Kingston, ON, K7L 3N6, Canada.
Email: magoski@queensu.ca

**Abstract figure legend** In the neuroendocrine bag cell neurons of the sea snail *Aplysia*, a non-selective cation channel drives activity and the secretion of reproductive hormone. The reactive oxygen species, $H_2O_2$, opens this channel and depolarizes the neurons. We now demonstrate that the phosphoinositide metabolites diacylglycerol (DAG) and inositol trisphosphate ($IP_3$), which are generated when phospholipase C (PLC) cleaves phosphatidylinositol-4,5-bisphosphate ($PIP_2$), act in concert with $H_2O_2$ to not only cause depolarization, but also result in physiological bursting.

## Key points

- *Aplysia* bag cell neurons secrete reproductive hormone during a lengthy burst of action potentials, known as the afterdischarge.
- During the afterdischarge, phospholipase C (PLC) hydrolyses phosphatidylinositol-4,5-bisphosphate into diacylglycerol (DAG) and inositol trisphosphate ($IP_3$). Subsequent activation of protein kinase C (PKC) leads to $H_2O_2$ production.
- $H_2O_2$ evokes a voltage-dependent inward current and action potential firing.
- Both a DAG analogue, 1-oleoyl-2-acetyl-*sn*-glycerol (OAG), and $IP_3$ enhance the $H_2O_2$-induced current, which is mimicked by the PLC activator, *N*-(3-trifluoromethylphenyl)-2,4,6-trimethylbenzenesulfonamide.
- The frequency of $H_2O_2$-evoked afterdischarge-like bursting is augmented by OAG or OAG plus $IP_3$.
- Stimulating PKC with phorbol 12-myristate 13-acetate shortens the latency and increases the duration of $H_2O_2$-induced bursts.
- The nicotinamide adenine dinucleotide phosphate oxidase inhibitor, 3-benzyl-7-(2-benzoxazolyl) thio-1,2,3-triazolo[4,5-d]pyrimidine, attenuates burst firing in bag cell neuron clusters.

## Introduction

Hydrogen peroxide ($H_2O_2$) is a reactive oxygen species produced by dismutation of the superoxide anion, $O_2^{\bullet-}$, which is generated by either the electron transport chain (Boveris & Chance, 1973; Brookes *et al.* 2004) or nicotinamide adenine dinucleotide phosphate oxidase (NOX) (Babior *et al.* 1973; Royer-Pokora *et al.* 1986; Bedard & Krause, 2007). Although typically associated with pathology, $H_2O_2$ can modulate ion channels (Bychkov *et al.* 1999), including non-selective cation channels in striatal (Hill *et al.* 2006), hippocampal (Olah *et al.* 2009) and nigral (Lee *et al.* 2013) neurons, as well as heterologously expressed canonical (Graham *et al.* 2010) or melastatin (Tong *et al.* 2006) transient receptor potential (TRP) channels.

Cation channels influence bursting or persistent firing of numerous neurons (Siemen & Hescheler, 1993; Partridge *et al.* 1994; Flockerzi, 2004), such as those in olfactory bulb (Dong *et al.* 2009) and hypothalamus (Ghamari-Langroudi & Borque, 2002), as well as entorhinal (Shalinsky *et al.* 2002), hippocampal (Knauer *et al.* 2013) and prefrontal cortex (Sidiropoulou *et al.* 2009). Along with voltage (Kononenko *et al.* 2004), intracellular $Ca^{2+}$ (Yellen, 1982; Partridge *et al.* 1994) and phosphorylation (Magoski & Kaczmarek, 2004), cation channels are controlled by plasma membrane lipids and their metabolites (Hofmann *et al.* 1999; Albert & Large, 2003; Hardie, 2007; Svobodova & Groschner, 2016). The present study concerns phosphoinositide regulation of an $H_2O_2$-gated cation channel in bag cell neurons from the marine mollusc *Aplysia californica*.

Bag cell neurons are electrically coupled neuroendocrine cells that trigger reproduction (Kupfermann, 1967; Conn & Kaczmarek, 1989; Sturgeon & Magoski, 2018). Following a brief cholinergic synaptic input, these neurons afterdischarge, where all cells depolarize and fire synchronous action potentials (Kupfermann & Kandel, 1970; White & Magoski, 2012; Dargaei *et al.* 2014). The afterdischarge has an ∼5 Hz, ∼1 min fast phase, followed by an ∼1 Hz, ∼30 min slow phase, and leads to the neurohaemal secretion of egg-laying hormone (Arch, 1972; Pinsker & Dudek, 1977; Kaczmarek *et al.* 1982; Loechner *et al.* 1990; Michel & Wayne, 2002). During the slow phase, the phosphoinositide-specific phosphodiesterase, phospholipase C (PLC), cleaves phosphatidylinositol 4,5-bisphosphate ($PIP_2$) into inositol trisphosphate ($IP_3$) and diacylglycerol (DAG) (Fink *et al.* 1988), with DAG then activating PKC (Takai *et al.* 1979; Wayne *et al.* 1999). In turn, PKC generates $H_2O_2$, potentially by phosphorylation of NOX cytosolic regulatory subunit, $p47^{phox}$, which co-localizes with membrane-bound NOX2 (Fontayne *et al.* 2002; Munnamalai *et al.* 2014).

A conductance that is fundamental to propelling the afterdischarge is a voltage-gated cation channel (Wilson *et al.* 1996; Magoski *et al.* 2002; Lupinsky & Magoski, 2006; Geiger *et al.* 2009). We previously found that $H_2O_2$ triggers this channel to evoke a voltage-dependent inward current capable of eliciting afterdischarge-like responses in cultured bag cell neurons or whole clusters (Chauhan & Magoski, 2019). Prior single-channel recordings in excised, inside-out patches showed that the cation channel is enhanced by exogenous DAG plus $IP_3$, or direct activation of endogenous PLC (Sturgeon & Magoski, 2018). Since phosphoinositide metabolism and $H_2O_2$ production occur in relatively close succession during the afterdischarge, these messengers may act in concert on the channel to maintain bursting. Here, we test this possibility, and find that the $H_2O_2$-induced current is augmented by a synthetic DAG analogue as well as a PLC activator. Moreover, a combination of synthetic DAG plus $IP_3$ further amplifies both the current and action potential firing brought about by $H_2O_2$.

Phospholipids modulate ion channels associated with pain (Hansen, 2015), sensory processing (Hille *et al.* 2015) and neuroendocrine function (Wen *et al.* 2012). Meanwhile, $H_2O_2$ boosts excitability in both *Aplysia* sensory neurons (Chang *et al.* 2003) and guinea pig substantia nigra neurons (Lee *et al.* 2011), as well as enhancing synaptic transmission in the rat ventral horn (Ohashi *et al.* 2016). Our findings in bag cell neurons link these two regulatory pathways with implications for reproduction.

## Methods

### Animals, ethical approval and cell culture

Adult *Aplysia californica* (a hermaphrodite) weighing 200–650 g were obtained from Marinus (Long Beach, CA, USA), housed in an ∼300 litre aquarium containing continuously circulating, aerated sea water (Instant Ocean; Aquarium Systems, Mentor, OH, USA) at 16–18°C on a 12:12 h light–dark cycle, and fed romaine lettuce five times/week. All experiments were approved by the Queen's University Animal Care Committee (protocols 2013-041 and 2017-1745).

For primary cultures of isolated bag cell neurons, animals were anaesthetized by an injection of isotonic $MgCl_2$ (390 mM; volume ∼50% of body weight), and the abdominal ganglion was removed and treated with dispase II (13.3 mg/ml; 04942078601; Roche Diagnostics/Sigma-Aldrich, Oakville, ON, Canada) dissolved in tissue culture artificial sea water (tcASW) (composition in mM: 460 NaCl, 10.4 KCl, 11 $CaCl_2$, 55 $MgCl_2$, 15 HEPES, 1 mg/ml glucose, 100 U/ml penicillin plus 0.1 mg/ml streptomycin (P4333; Sigma-Aldrich); pH 7.8 with NaOH) for 18 h at 22°C. The remainder of the nervous system was also removed and disposed to achieve euthanasia. The abdominal ganglion was then rinsed in tcASW for 1 h, and fine scissors and

forceps were used to micro-dissect the bag cell neuron clusters from their surrounding connective tissue. These desheathed clusters were then either placed in tcASW in a 14°C incubator and used for intracellular recording the next day (see Methods, 'Sharp-electrode recording from bag cell neurons in isolated clusters' for details) or individual bag cell neurons were dissociated and dispersed in tcASW onto 35 × 10 mm polystyrene tissue culture dishes (353001; Falcon-Corning/Thermo Fisher Scientific; Ottawa, ON, Canada) using a fire-polished borosilicate-glass Pasteur pipette (13-678-30; Thermo Fisher Scientific) and gentle trituration. Cultures were placed in a 14°C incubator and used for experimentation within 1–3 days. Salts were obtained from Thermo Fisher Scientific, MP Biomedicals (Aurora, OH, USA), Acros Organics (Morris Plains, NJ, USA) or Sigma-Aldrich.

## Whole-cell voltage-clamp and current-clamp recording from cultured bag cell neurons

Recordings of current or membrane potential were performed at room temperature (20–22°C) using an EPC-8 amplifier (HEKA Electronik/Harvard Apparatus; Saint-Laurent, QC, Canada) and the tight-seal, whole-cell method (Hamill *et al*. 1981). Microelectrodes were pulled from 1.5-/1.12-mm external-/internal-diameter borosilicate-glass capillaries (TW150F-4; World Precision Instruments, Sarasota, FL, USA) and had a resistance of 1–2 MΩ when filled with intracellular saline (see below). Pipette junction potentials were nulled immediately before seal formation; after making a seal, pipette capacitive currents were cancelled. Following membrane rupture, neuronal capacitive currents were cancelled and the series resistance (3–5 MΩ) was compensated to 70–80% and monitored throughout the experiment. Current was low-pass filtered at 1 kHz with the variable EPC-8 Bessel filter and sampled at 2 kHz using a Digidata 1322A analog-to-digital converter (Molecular Devices, Sunnyvale, CA, USA), the Clampex acquisition program of pCLAMP v8.1 (Molecular Devices), and an IBM-compatible personal computer. Voltage-clamp holding potential (see Results for details) was set using Clampex. For current-clamp, voltage was low-pass filtered with a dedicated 5 kHz Bessel filter on the EPC-8 and sampled as per current; in addition, using constant bias current from the EPC-8 V-Hold, the membrane potential was initially set to −40 mV, which is typical for the slow phase of the afterdischarge (Kaczmarek *et al*. 1982; White & Magoski, 2012).

All recordings were made in normal artificial sea water (nASW; composition as per tcASW but lacking glucose and antibiotics). For voltage-clamp, a $Cs^+$-based intracellular saline (composition in mM: 500 $Cs^+$-Asp, 70 KCl, 1.25 $MgCl_2$, 10 HEPES, 11 glucose, 10 glutathione, 5 EGTA, 5 ATP-2Na·$H_2O$ (A3377; Sigma-Aldrich) and 0.1 GTP-Na·$H_2O$ (G8877; Sigma-Aldrich); pH 7.3 with KOH) was used. For current-clamp, a $K^+$-based intracellular saline (composition, as per the $Cs^+$-based saline, but with $K^+$ replacing $Cs^+$) was used. For both intracellular salines, as calculated using WebMaxC (https://somapp.ucdmc.ucdavis.edu/pharmacology/bers/maxchelator/webmaxc/webmaxcS.htm), 3.75 mM $CaCl_2$ was added to set the free $Ca^{2+}$ concentration at 300 nM, which corresponds to the approximate resting intracellular $Ca^{2+}$ concentration of bag cell neurons (Loechner *et al*. 1992; Fisher *et al*. 1994; Magoski *et al*. 2000). Junction potentials of 17 and 15 mV were calculated for the $Cs^+$- and $K^+$-based intracellular salines, respectively, *vs*. nASW and compensated for by subtraction off-line. Given that the junctional potential was nulled prior to seal formation (see above), once whole-cell mode was established, the holding potential was given by the command potential (from Clampex) minus the junction potential.

## Sharp-electrode recording from bag cell neurons in isolated clusters

Sharp-electrode recordings from bag cell neurons in clusters were carried out using a Neuroprobe 1600 amplifier (A-M Systems; Sequim, WA, USA) at room temperature (20–22°C) in nASW. Microelectrodes were pulled from 1.2-/0.9-mm external/internal-diameter, borosilicate-glass capillaries (TW120F-4; World Precision Instruments), and had a resistance of 10–20 MΩ when filled with 2 M potassium acetate plus 10 mM HEPES and 100 mM KCl (pH 7.3 with KOH). A Grass S88 stimulator was used to deliver 50 ms hyperpolarizing current pulses to balance the bridge as well as inject trains of 50 ms depolarizing current pulses to evoke action potentials. Voltage was filtered at 5 kHz using the Neuroprobe variable low-pass filter and acquired with the Digidata and Axoscope 9.0 (Molecular Devices) at 2 kHz.

## Drug application and reagents

Solution exchanges were accomplished using a calibrated transfer pipette to replace the bath (culture dish) tcASW with nASW prior to the start of an experiment. For extracellular application of drugs, most reagents were introduced before or during recording by initially removing a small volume (∼50 $\mu$l) of saline from the bath, combining that with ≤10 $\mu$l of drug stock solution (see below), and then re-introducing that mixture back into the bath. Care was taken to pipette near the side of the dish and as far away as possible from the neuron. An exception was application of acetylcholine to isolated clusters, which was achieved by pressure-ejection from a PMI-100 pressure ejector (Dagan; Tucson, AZ, USA) using 10-s,

75–100 kPa pulses and an unpolished whole-cell pipette (1–2 $\mu$m tip diameter) positioned ∼50 $\mu$m away from the cluster. For intracellular application, which was necessary for membrane-impermeable $IP_3$ and heparin, stocks were diluted down to final concentration in intracellular saline and delivered to the neuron via the whole-cell electrode during recording.

Water was used to dissolve the following as stocks at the indicated concentrations: hydrogen peroxide ($H_2O_2$; 200 mM; H325-500; Thermo Fisher Scientific), D-*myo*-inositol 1,4,5-trisphosphate trisodium salt ($IP_3$; 10008205; Cayman Chemicals, Ann Arbor, MI, USA), heparin (2 mM; H3393; Sigma-Aldrich) and acetylcholine (10 mM; A6625; Sigma-Aldrich). Similarly, dimethyl sulfoxide (DMSO; BP231-1; Thermo Fisher Scientific) was used to dissolve the following: 1-oleoyl-2-acetyl-*sn*-glycerol (OAG; 25 mM; O6754; Sigma-Aldrich or 62600; Cayman), *N*-(3-trifluoromethylphenyl)-2,4,6-trimethylbenzenesulfonamide (*m*-3M3FBS; 25 mM; T5699; Sigma-Aldrich or 16867; Cayman), *N*-(2-trifluoromethylphenyl)-2,4,6-trimethylbenzenesulfonamide (*o*-3M3FBS; 25 mM; 1942; Tocris Bioscience, Bristol, UK or 17251; Cayman), cyclopiazonic acid (CPA; 20 mM; 11326; Cayman), 4-$\alpha$-phorbol (10 mM; P4888; Sigma-Aldrich), phorbol 12-myristate 13-acetate (PMA; 10 mM; 79346; Sigma-Aldrich) and 3-benzyl-7-(2-benzoxazolyl)thio-1,2,3-triazolo[4,5-d]pyrimidine (VAS2870; 5 mM; 19205; Cayman). The final concentration of DMSO was ≤0.2% (v/v), which in control experiments, here or in prior studies, had no effect on bag cell neuron holding current, membrane conductance or membrane potential (Hickey *et al.* 2010; Tam *et al.* 2011; Sturgeon & Magoski, 2016; White *et al.* 2018).

### Analysis

The Clampfit analysis program of pCLAMP was used to determine the amplitude of changes to membrane current or potential evoked by $H_2O_2$ or other reagents under voltage- or current-clamp. For peak change, two cursors were placed 30 s apart, 30 s prior to drug addition, and the average between the cursors served as a baseline. An additional two cursors were placed 60 s apart on either side of the peak of the response. Clampfit then calculated the peak amplitude relative to the baseline. To determine cell viability in the presence of OAG, the percentage recovery of the current following a response was determined by comparing the peak current to the steady-state current, the latter being calculated by again placing two cursors, 30 s apart, at the end of the trace, well after the peak and where the response had recovered to steady-state. For display only, some current traces were filtered off-line to between 50 and 100 Hz using the Clampfit Gaussian filter. Due to the overall slow nature of the responses, this second filtering brought about no change in amplitude or kinetics. Reversal potential involved taking a difference current, ascertained by subtracting the current elicited by a voltage ramp from −60 to +60 mV before drug application, from the current elicited by the same ramp at the peak of the subsequent drug response. The reversal potential was then measured directly from where the difference current crossed the *x*-axis. For responses recorded under current-clamp that presented with robust spiking, which made it difficult to visualize the peak depolarization, Clampfit was used to generate all-points histograms for before and after $H_2O_2$ application. The largest peaks of the resulting histograms were fit in Clampfit with a Gaussian function by the least-squares method and a simplex search, and taken as the average membrane potential. The difference between the voltage before and after $H_2O_2$ served as the amplitude of the depolarization. To determine firing frequency in $H_2O_2$, the number of spikes during the response was determined using the Clampfit threshold search function, and divided by the total time of the burst.

Data are means ± standard deviation with individual data points overlaid. Statistical analysis was performed using InStat v3.1 or Prism v8.0 (both GraphPad Software Inc.; La Jolla, CA, USA). The Kolmogorov–Smirnov method was used to test data sets for normality. To test whether the mean differed between two groups of normally distributed data, Student's unpaired *t*-test was used, whereas for non-normally distributed data, the Mann–Whitney *U*-test was used. For three groups, an ordinary one-way analysis of variance (ANOVA) with either the Dunnett multiple comparisons or Tukey–Kramer multiple comparisons test was used. Means were considered significantly different if the two-tailed *P*-value was $<0.05$ and are indicated on graphs with an asterisk. All *P*-values are given in full.

## Results

### $H_2O_2$ activates a prolonged, inward current and induces action potential firing in cultured bag cell neurons

Our prior work showed that $H_2O_2$ activates a non-selective cation channel to elicit a long-lasting voltage-dependent cationic current in bag cell neurons (Chauhan & Magoski, 2019). This was confirmed here using single cultured bag cell neurons and whole-cell voltage-clamp (see Methods, 'Whole-cell voltage-clamp and current-clamp recording from cultured bag cell neurons' for details). Neurons were bathed in $Na^+$-containing nASW (used throughout) and dialysed

with $Cs^+$-Asp-based intracellular saline (to block $K^+$ channels as well as improve current resolution and stability) in the pipette for 15 min while holding at −60 or −30 mV. As per our earlier findings (Chauhan & Magoski, 2019), the voltage-dependence of the $H_2O_2$-induced response resulted in minimal current at −60 mV (∼−50 pA; $n = 6$) and a significantly larger current at −30 mV (∼−120 pA; $n = 9$) (Fig. 1*A* and *B*); the latter holding potential was chosen for all subsequent voltage-clamp experiments.

In keeping with gating a cation current, $H_2O_2$ elicited prolonged action potential firing from whole-cell current-clamped cultured bag cell neurons bathed in nASW with $K^+$-Asp-based intracellular saline, that is, physiological conditions. We verified our past report (Chauhan & Magoski, 2019) that bath-application of 1 mM $H_2O_2$ to a neuron set to a resting potential of −40 mV, the average membrane potential during the afterdischarge, caused an ∼9 mV depolarization and consistently generated an afterdischarge-like burst of spikes ($n = 10$) (Fig. 1*C* and *D*).

## The $H_2O_2$-induced current is enhanced by a DAG analogue

Once the cholinergic input starts the afterdischarge, a currently unknown mechanism activates phospholipase C early in the slow phase, which results in the liberation of $IP_3$ and DAG from $PIP_2$ (Fink *et al.* 1988; Conn *et al.* 1989; White & Magoski, 2012). PKC is then activated by DAG (Wayne *et al.* 1999), which stimulates $H_2O_2$ production (Munnamalai *et al.* 2014). We previously showed that a synthetic DAG analogue, 1-oleoyl-2-acetyl-*sn*-glycerol (OAG), gates a voltage-*independent* cation channel at the whole-cell level (Sturgeon & Magoski, 2016). In addition, we demonstrated that OAG enhances the activity of a different, voltage-*dependent* cation channel in cell-free patches (Sturgeon & Magoski, 2018). Our prior work also indicates that the $H_2O_2$-induced macroscopic current is biophysically and pharmacologically the same as the voltage-dependent cation conductance observed at the single-channel level (Chauhan & Magoski, 2019). Thus, we tested whether the $H_2O_2$-induced cation current is similarly augmented by phosphoinositide metabolites in cultured bag cell neurons.

With $Cs^+$-Asp-based saline in the pipette and at a holding potential of −30 mV, bath-application of 0.1% (v/v) DMSO (the vehicle for OAG), produced minimal, typically outward current (∼+65 pA; $n = 5$) (Fig. 2*A* and *C*). Delivery of 1 mM $H_2O_2$ in the presence of DMSO generated an inward current of ∼−80 pA ($n = 5$) (Fig. 2*A* and *D*, left). By comparison, and in keeping with our previously reported outcome (Sturgeon & Magoski, 2016), introduction of 25 $\mu$M OAG on its own resulted in a noisy inward current of ∼−2.3 nA that was significantly larger than DMSO alone ($n = 6$) (Fig. 2*B* and *C*). Moreover, we now observed that the presence of OAG

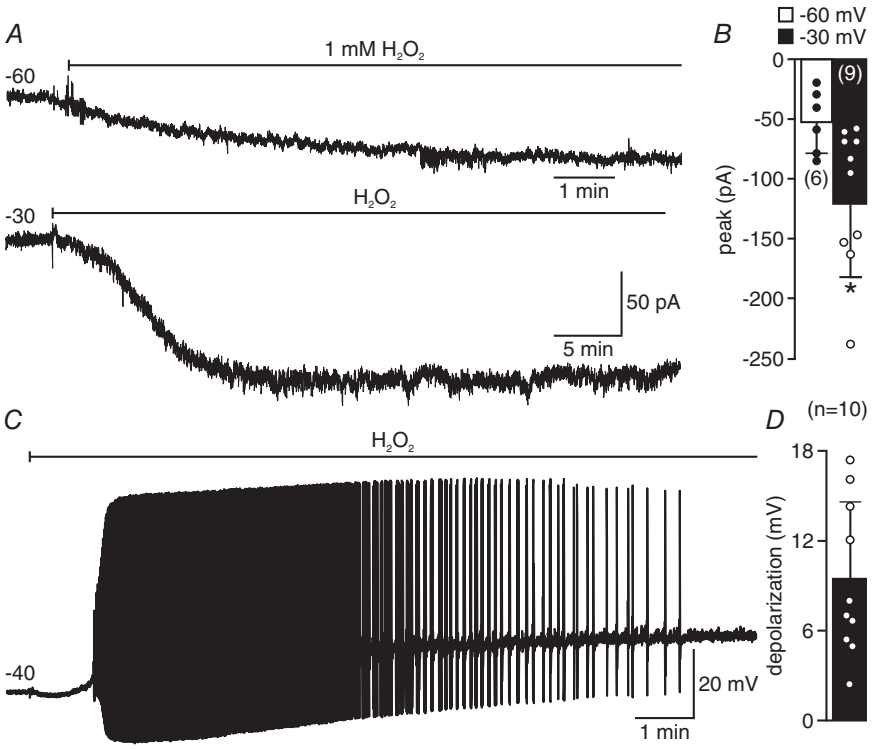


**Figure 1. $H_2O_2$ evokes an inward current and action potential firing**
*A*, whole-cell voltage-clamp recordings from two, separate cultured bag cell neurons held at −60 (top; holding current ($I_{hold}$) = −189.9 pA) and −30 mV (bottom; $I_{hold}$ = −70.7 pA) in nASW with $Cs^+$-Asp-based intracellular saline revealing a relatively small, inward current at −60 mV and a larger, slowly inactivating current at −30 mV in response to 1 mM bath-applied $H_2O_2$ (at bar). Ordinate applies to both traces. *B*, group data showing that peak $H_2O_2$-induced currents at −60 (−52.5 ± 26.2 pA) and −30 mV (−120.5 ± 60.9 pA) are significantly different ($t_{(13)}$ = 2.559; $P$ = 0.0238; unpaired Student's *t*-test). *C*, voltage response to $H_2O_2$ of a different bag cell neuron whole-cell current-clamped in nASW with $K^+$-Asp-based intracellular saline and initially set to −40 mV with bias current. Introduction of 1 mM $H_2O_2$ depolarized the membrane potential and induced an ∼10 min burst of action potentials. *D*, summary graph indicating the average $H_2O_2$-evoked depolarization from −40 mV (9.4 ± 5.2 mV).

also significantly augmented the $H_2O_2$-induced current by ∼170% to ∼−220 pA ($n$ = 9) (Fig. 2*B* and *D*, left). The onset latency of the $H_2O_2$-induced current was similar in both control and OAG, at 12–14 s (Fig. 2*D*, middle).

Usually, the $H_2O_2$-induced current had fairly uniform and smooth kinetics at a holding potential of −30 mV; however, in the presence of OAG, the response to $H_2O_2$ was noisy. Reports in the literature, including from our own laboratory, show that OAG-induced currents often include large, rapid deflections with an increase in noise (Helliwell & Large, 1997; Albert & Large, 2003; Sturgeon & Magoski, 2016). Thus, we tested for cell viability by examining the percentage recovery of the $H_2O_2$-induced current in the presence of DMSO (∼45%; $n$ = 5) *vs*. OAG (∼70%; $n$ = 6) (Fig. 2*D*, right). There was no significant difference in the percentage recovery, suggesting that exposure to OAG did not cause pathology.

## OAG and $IP_3$ synergistically boost the $H_2O_2$-induced current

During the afterdischarge, DAG and $IP_3$ levels are expected to rise concurrently (Fink *et al*. 1988). While neither ourselves nor others have found that intracellular delivery of $IP_3$ alone causes bag cell neurons to depolarize (Fink *et al*. 1988; Sturgeon & Magoski, 2016), we have observed that $IP_3$ further enhances the upregulation of the voltage-dependent cation current brought about by OAG at the single-channel level (Sturgeon & Magoski, 2018). Hence, we next investigated the effect of $IP_3$ or OAG plus $IP_3$ on the $H_2O_2$-induced current. Cultured neurons were voltage-clamped at −30 mV and perfused intracellularly (aka dialysed) for 15 min via the pipette with either $Cs^+$-Asp-based intracellular saline alone or saline containing 5 $\mu$M $IP_3$. Delivery of 1 mM $H_2O_2$ to control cells elicited an inward current of ∼−95 pA

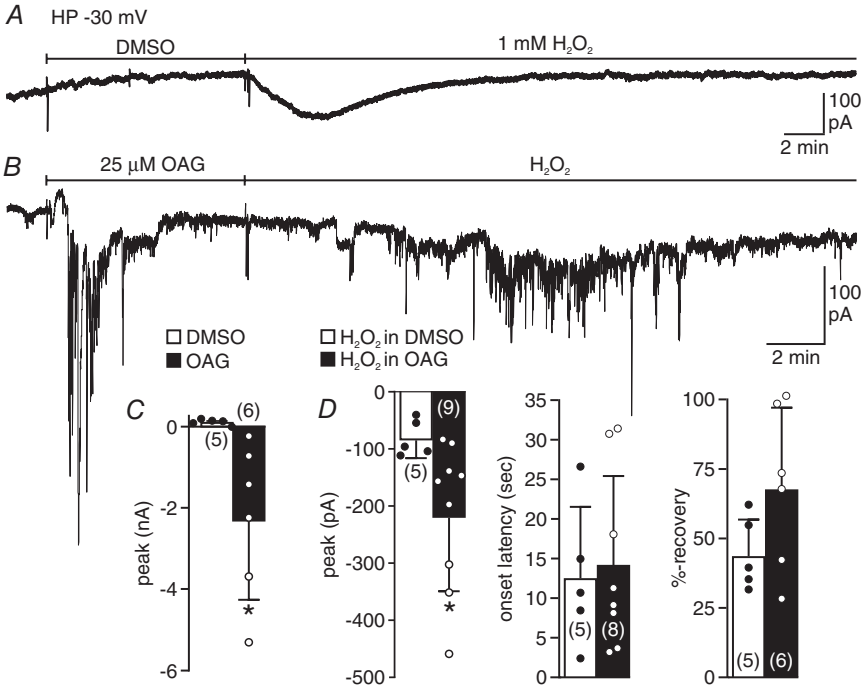


**Figure 2. A diacylglycerol analogue enhances the $H_2O_2$-induced current**
*A*, cultured bag cell neurons were voltage-clamped at a holding potential (HP) of −30 mV using $Cs^+$-Asp-based intracellular saline in the pipette and nASW in the bath. Delivery of the vehicle, 0.1% (v/v) DMSO (at bar), elicits a small outward current (initial $I_{hold}$ = −147.5 pA). The addition of 1 mM $H_2O_2$ in the presence of DMSO caused a typical inward current. *B*, bath-application of 25 $\mu$M 1-oleoyl-2-acetyl-*sn*-glycerol (OAG), a diacylglycerol analogue, caused a large, noisy inward current (initial $I_{hold}$ = −104.8 pA). Introduction of $H_2O_2$ ∼30 min after OAG application produced an inward current that was both noisy and greater than $H_2O_2$ in DMSO. *C*, summary data representing a significant difference in the peak currents following DMSO (62.8 ± 77.4 pA) *vs*. OAG (−2.3 ± 1.9 nA) ($U_{5,6}$ = 0; $P$ = 0.0043; Mann–Whitney *U*-test). *D*, average data illustrating a significant increase in the $H_2O_2$-induced peak current (−217.4 ± 129.5 pA) post-OAG in contrast to the response generated by $H_2O_2$ after DMSO (−81.0 ± 31.4 pA) ($U_{5,9}$ = 5.0; $P$ = 0.0190; Mann–Whitney *U*-test) (left). However, for DMSO *vs*. OAG, there was no significant difference in either the onset latency (middle; 12.6 ± 9.1 *vs*. 14.0 ± 11.3 s; $t_{(11)}$ = 0.2799; $P$ = 0.7847; unpaired Student's *t*-test) or percentage recovery (right; 44.1 ± 13.1% *vs*. 67.4 ± 29.3%; $t_{(9)}$ = 1.638; $P$ = 0.1359; unpaired Student's *t*-test) of the $H_2O_2$-induced current.

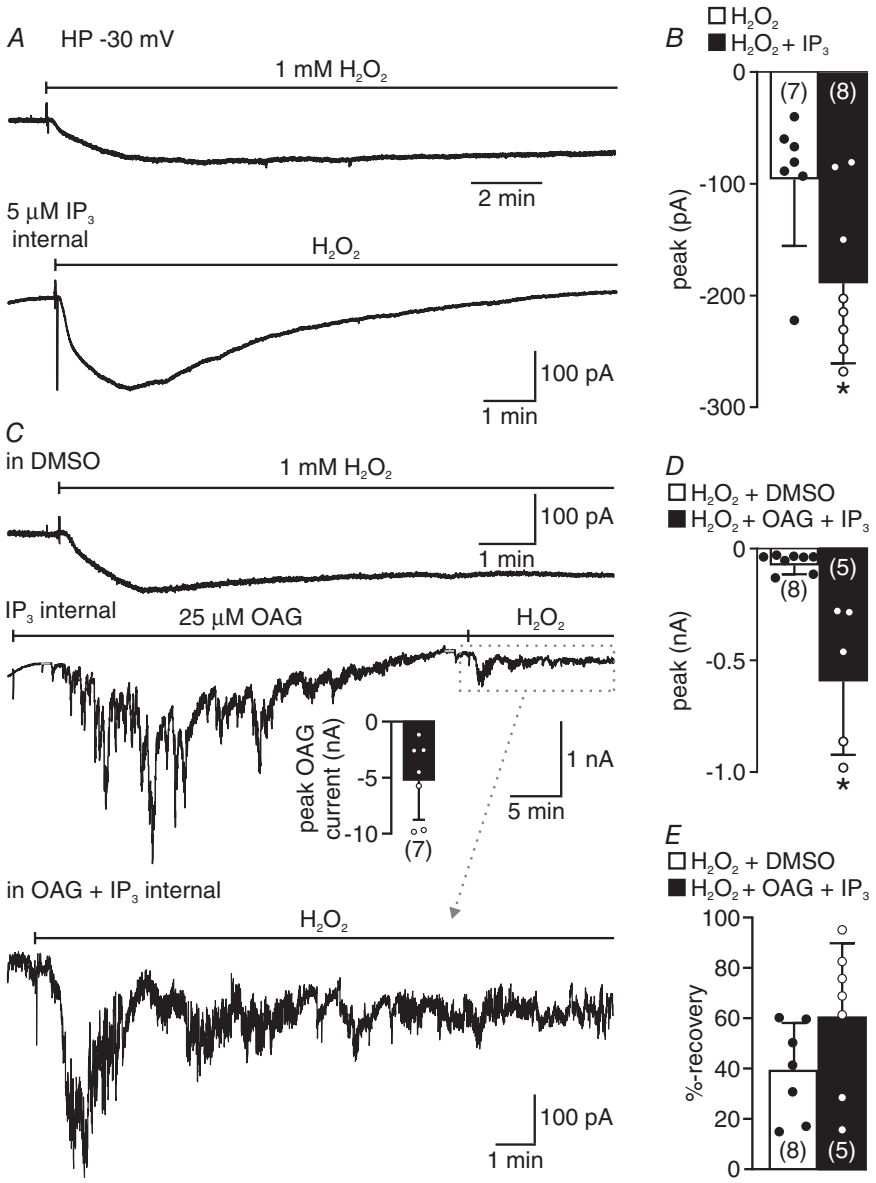


**Figure 3. $IP_3$ or OAG plus $IP_3$ further augments the $H_2O_2$-induced current**
*A*, cultured bag cell neurons under voltage-clamp at −30 mV with or without 5 $\mu$M intracellular $IP_3$. In a control cell dialysed with $Cs^+$-Asp-based saline alone, 1 mM $H_2O_2$ (at bar) elicited a characteristic inward current (top; $I_{hold} = -77.1$ pA). By comparison, dialysis with saline containing $IP_3$ followed by $H_2O_2$ induced a greater response (bottom; $I_{hold} = -109.6$ pA). Ordinate applies to both traces. *B*, group data confirming a significant increase in the $H_2O_2$-induced current in the presence (−187.7 ± 71.9 pA) *vs*. the absence (−94.8 ± 59.8 pA) of $IP_3$ ($U_{7,8} = 9.0$; $P = 0.0289$; Mann–Whitney *U*-test). *C*, representative response to $H_2O_2$ in the presence of the vehicle, DMSO, in a neuron dialysed with intracellular saline alone (top; $I_{hold} = +3.3$ pA). When $IP_3$ was in the pipette, delivery of 25 $\mu$M OAG caused a large and noisy inward current (−5.2 ± 3.5 nA; inset); when $H_2O_2$ was applied ∼30 min later, the evoked current was markedly enhanced compared to control (middle; initial $I_{hold} = -556.6$ pA). The dashed box around the $H_2O_2$-induced current in the presence of OAG plus $IP_3$ is shown magnified (bottom). *D*, summary data revealing that, in comparison to DMSO (−68.6 ± 39.9 pA), the presence of OAG plus $IP_3$ significantly elevated the $H_2O_2$-induced current (−588.0 ± 328.2 pA) ($U_{5,8} = 0$; $P = 0.0016$; Mann–Whitney *U*-test). There was also a significant increase from the $H_2O_2$-induced current in the presence of $IP_3$ alone to OAG plus $IP_3$ (comparison of black bars in *B* and *D*; $U_{(8,5)} = 0$; $P = 0.0016$; Mann–Whitney *U*-test). *E*, there was no significant difference in the percentage recovery of the $H_2O_2$-induced current with DMSO (39.6 ± 18.9%) or OAG plus $IP_3$ (61.1 ± 29.1%) in the bath ($t_{(12)} = 2.374$; $P = 0.1264$; unpaired Student's *t*-test).

($n = 7$) (Fig. 3*A*, top, and *B*), whereas dialysis with $IP_3$ resulted in a significantly larger $H_2O_2$-induced current of ∼−190 pA ($n = 8$) (Fig. 3*A*, bottom, and *B*).

Next, we studied the impact of OAG plus $IP_3$ on the response to $H_2O_2$. In a previous report, we noted that the addition of $IP_3$ increased the voltage-independent cation current opened by OAG alone (Sturgeon & Magoski, 2016); thus, in the present study we waited for that response to subside before adding $H_2O_2$. For control, neurons were voltage-clamped at −30 mV and dialysed for 15 min. Bath-application of 1 mM $H_2O_2$ in the presence of DMSO produced a response of ∼−70 pA ($n = 8$) (Fig. 3*C*, top, and *D*). With inclusion of 5 $\mu$M $IP_3$ in

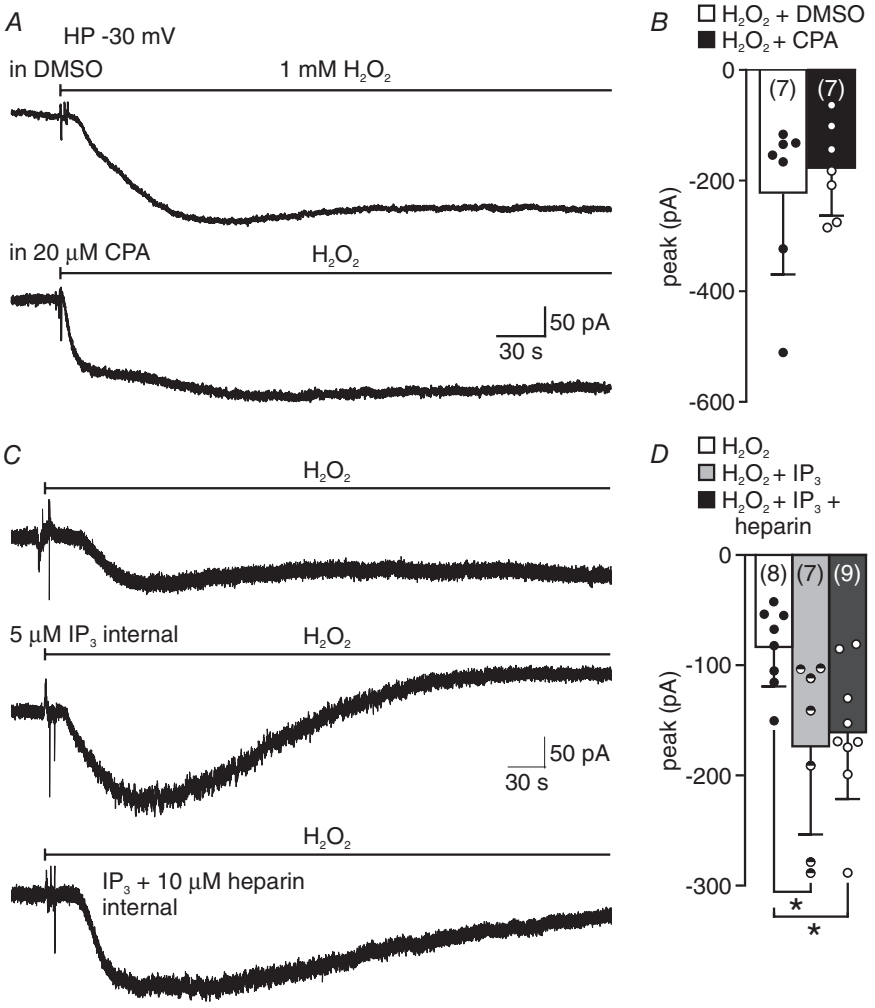


**Figure 4. $IP_3$-mediated regulation of the $H_2O_2$-induced current does not appear to involve intracellular $Ca^{2+}$ stores**
*A*, different cultured bag cell neurons were voltage-clamped at −30 mV. Bath-application of 1 mM $H_2O_2$ (at bar) following DMSO delivery produced an expected inward current (top; $I_{hold} = +285.4$ pA). When 20 $\mu$M of the endoplasmic reticulum $Ca^{2+}$ pump blocker CPA was first given for ∼15 min, the subsequent addition of $H_2O_2$ resulted in a response that was similar to control (bottom; $I_{hold} = −44.0$ pA). Scale bars apply to both traces. *B*, average data showing no significant difference for the $H_2O_2$-induced current in DMSO (−223.1 ± 146.0 pA) *vs.* CPA (−180.8 ± 84.8 pA) ($U_{7,7} = 21.0$; $P = 0.7104$; Mann–Whitney *U*-test). *C*, separate neurons voltage-clamped at −30 mV with $Cs^+$-Asp-based intracellular saline alone, with 5 $\mu$M $IP_3$, or with $IP_3$ plus 10 $\mu$M heparin in the pipette. As expected, compared to the control 1 mM $H_2O_2$ (at bar) response (top; $I_{hold} = +144.2$ pA), dialysis with $IP_3$ potentiated the $H_2O_2$-induced current (middle; $I_{hold} = −72.8$ pA); moreover, the presence of heparin, an $IP_3$ receptor blocker, failed to prevent the $IP_3$-mediated enhancement (bottom; $I_{hold} = −93.4$ pA). Scale bars apply to all traces. *D*, summary data revealing that while the inclusion of $IP_3$ significantly increased the $H_2O_2$-induced current (−173.7 ± 81.2 pA) *vs.* control (−83.9 ± 37.0 pA), this elevation was not counteracted by intracellular heparin (−160.9 ± 62.4 pA) ($F_{2,21} = 4.844$, $P = 0.0186$, standard ANOVA; $P < 0.05$ Tukey–Kramer multiple comparisons test).

the intracellular saline, the initial application of 25 $\mu$M OAG evoked a large, ∼−5 nA inward current, which again is similar to our earlier work ($n$ = 7) (Fig. 3*C*, middle, inset) (Sturgeon & Magoski, 2016). Moreover, compared to DMSO, the presence of OAG plus $IP_3$ significantly augmented the subsequent $H_2O_2$-induced current by ∼750% to ∼−590 pA ($n$ = 5) (Fig. 3*C*, middle dashed-box, bottom, and *D*). As seen in OAG alone, the $H_2O_2$-induced current was noisy; however, the extent of recovery of the $H_2O_2$ response was not significantly different between DMSO and OAG plus $IP_3$ (Fig. 3*E*).

$IP_3$ is an agonist of $Ca^{2+}$ release receptors on endoplasmic reticulum (Streb *et al.* 1983; Berridge & Irvine, 1989), including in bag cell neurons (Fink *et al.* 1988; Jonas *et al.* 1997). We controlled for the possibility that $Ca^{2+}$ release contributed to the $IP_3$-mediated enhancement of the $H_2O_2$-induced current by liberating $Ca^{2+}$ with cyclopiazonic acid (CPA). This reagent blocks the $Ca^{2+}$-ATPase on the endoplasmic reticulum, causing $Ca^{2+}$ to leak out of the store (Seidler *et al.* 1989). Treating with 20 $\mu$M CPA for ∼15 min, a period sufficient to elevate bag cell neuron intracellular $Ca^{2+}$ (Kachoei *et al.* 2006; Geiger & Magoski, 2008; Groten *et al.* 2013), did not significantly alter the current generated by 1 mM $H_2O_2$ ($n$ = 7) compared to that elicited in DMSO control conditions ($n$ = 7) (Fig. 4*A* and *B*). To further rule out involvement of intracellular stores, the $IP_3$ receptor blocker heparin (Ghosh *et al.* 1988) was employed. Neurons were voltage-clamped at −30 mV and loaded via the recording pipette for 15 min with $Cs^+$-Asp-based intracellular saline alone as control, intracellular saline with 5 $\mu$M $IP_3$, or intracellular saline with $IP_3$ plus 10 $\mu$M heparin. As expected, compared to the control 1 mM $H_2O_2$-induced current ($n$ = 8) (Fig. 4*C*, top), inclusion of $IP_3$ significantly enhanced the response by ∼100% ($n$ = 7) (Fig. 4*C*, middle, and *D*). Yet, the addition of heparin to the pipette did not prevent $IP_3$ from increasing the $H_2O_2$ response by ∼90% ($n$ = 9), which was not significantly different from $IP_3$ alone (Fig. 4*C*, bottom, and *D*).

## The $H_2O_2$-induced current is also enhanced by direct phospholipase C activation

An examination of lipid composition (Piomelli *et al.* 1987; Carlson & Levitan, 1990) and the liberation of DAG and $IP_3$ from $PIP_2$ by PLC (Fink *et al.* 1988) established the presence of phosphatidylinositides in *Aplysia* neuronal membranes. In addition, turning on PLC with the activator *m*-3M3FBS (Bae *et al.* 2003) released sufficient amounts of DAG and $IP_3$ to modulate the voltage-dependent cation channel in excised, inside-out patches from bag cell neurons (Sturgeon & Magoski, 2018). Thus, to compare with exogenous metabolite application, we examined the impact of PLC activation on the $H_2O_2$-induced current. Following an ∼15 min exposure to 25 $\mu$M of the inactive isoform, *o*-3M3FBS, delivery of 1 mM $H_2O_2$ evoked an inward current of ∼−130 pA ($n$ = 7) (Fig. 5*A*, top, and *B*, top). However, an ∼15 min treatment with 25 $\mu$M of the active isoform, *m*-3M3FBS, significantly boosted the

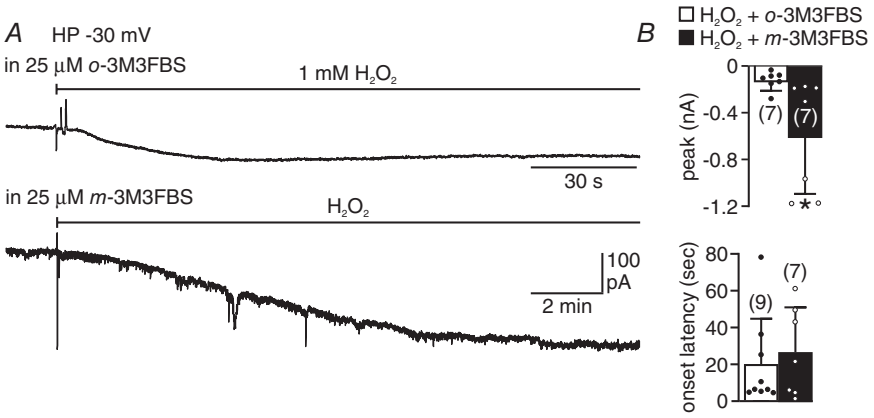


**Figure 5. Phospholipase C activation augments the $H_2O_2$-induced current**
*A*, voltage-clamp recording from a cultured bag cell neuron at −30 mV showing that bath-application of 1 mM $H_2O_2$ (at bar) after delivery of 25 $\mu$M of an inactive control molecule, *o*-3M3FBS (top; $I_{hold}$ = −143.0 pA), generated a typical inward current. In a separate neuron, adding 1 mM $H_2O_2$ in the presence of 25 $\mu$M of the PLC activator *m*-3M3FBS (bottom; $I_{hold}$ = −82.4 pA) amplified the $H_2O_2$-induced current. Ordinate applies to both traces. *B*, top, average data showing that neurons exposed to *m*-3M3FBS generated a significantly greater response to $H_2O_2$ (−598.3 ± 485.0 pA) compared to treatment with *o*-3M3FBS (−130.5 ± 78.6 pA) ($U_{7,7}$ = 3.0; $P$ = 0.0041; Mann–Whitney *U*-test). Bottom, there was no significant difference in the onset latency of the $H_2O_2$-induced current in the presence of *o*-3M3FBS (19.7 ± 24.7 s) *vs.* *m*-3M3FBS (26.2 ± 24.4 s) ($U_{7,9}$ = 30.0; $P$ = 0.9182; Mann–Whitney *U*-test).

$H_2O_2$-induced current to ∼−600 pA ($n$ = 7) (Fig. 5*A*, bottom, and *B*, top), but did not significantly alter the onset latency (∼20 s in *o*-3M3FBS *vs.* ∼26 s in *m*-3M3FBS) (Fig. 5*B*, bottom).

## OAG or OAG plus $IP_3$ increases the firing frequency of action potentials induced by $H_2O_2$

Having shown that the $H_2O_2$ response is enhanced by phosphoinositide metabolites, we sought to examine whether OAG plus $IP_3$ works in association with $H_2O_2$ to alter the membrane potential and evoke bursting. This was performed using current-clamp with $K^+$-Asp-based intracellular saline in the pipette. Cultured neurons were initially set to −40 mV, the typical membrane potential of the slow phase (Kaczmarek *et al.* 1982; White & Magoski, 2012), with bias current and exposed to DMSO followed by 1 mM $H_2O_2$ ∼50 s later (Fig. 6, top). The rationale for delivering $H_2O_2$ in short order was to mimic the time course of $H_2O_2$ production that would be expected after phosphoinositide turnover. Similar to our prior finding (Chauhan & Magoski, 2019), $H_2O_2$ application ($n$ = 8) resulted in a depolarization of 6.1 ± 3.1 mV accompanied by a burst of spikes at ∼0.55 Hz (Fig. 6, top, inset), with a duration of 6.1 ± 4.1 min and an onset latency of 1.8 ± 1.3 min. Next, we investigated the role of just OAG and $H_2O_2$ in influencing bag cell neuron activity. Delivery of 25 $\mu$M OAG and 1 mM $H_2O_2$ ($n$ = 5) in close succession caused neurons to depolarize by 6.5 ± 3.2 mV and fire action potentials at ∼1 Hz (Fig. 6, middle, inset) for 5.6 ± 2.4 min, with an onset latency of 2.6 ± 1.2 min. Finally, when neurons were dialysed with intracellular saline containing 5 $\mu$M $IP_3$ for 15 min, subsequent bath-application of 25 $\mu$M OAG and 1 mM $H_2O_2$ ($n$ = 9), again in close succession, generated a 5.0 ± 3.9 mV depolarization and a ∼0.95 Hz burst (Fig. 6, bottom, inset) of 7.6 ± 3.6 min, with an onset latency of 1.5 ± 0.6 min. The presence of either OAG or OAG

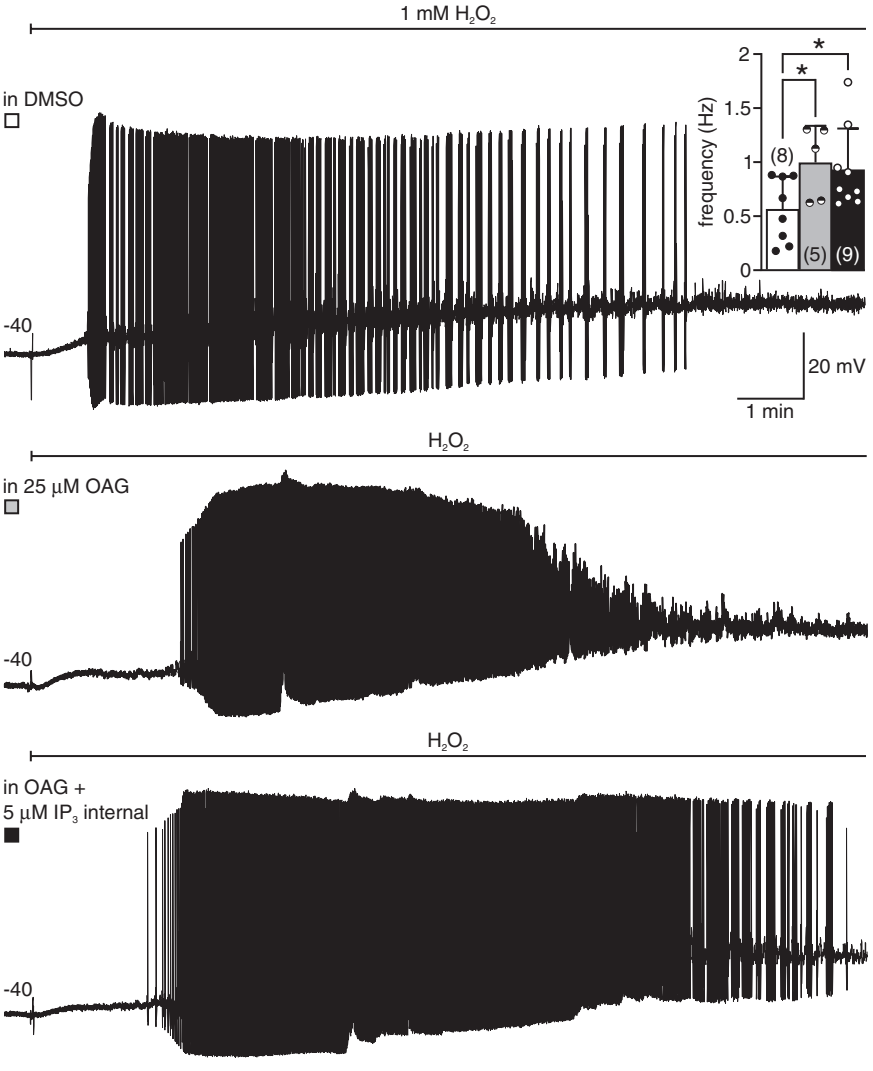


**Figure 6. OAG or OAG plus $IP_3$ elevates the frequency of action potentials evoked by $H_2O_2$**
Top, a cultured bag cell neuron was current-clamped in nASW with $K^+$-Asp-based intracellular saline and initially set to −40 mV with bias current. In the presence of DMSO, the delivery of 1 mM $H_2O_2$ (at bar) evoked depolarization and action potential firing. Middle, a separate neuron was first exposed to 25 $\mu$M OAG; delivery of 1 mM $H_2O_2$ 50 s later also resulted in action potentials, with a higher firing frequency compared to control. Bottom, a third neuron bathed in OAG was dialysed with 5 $\mu$M $IP_3$-containing intracellular saline. The addition of $H_2O_2$ again elicited more robust action potential firing *vs.* control. Scale bars apply to all traces. Inset, mean spike frequency in response to $H_2O_2$ in DMSO (white bar) (0.55 ± 0.30 Hz) differed significantly from both $H_2O_2$ in OAG (grey bar) (0.98 ± 0.34 Hz) and $H_2O_2$ in OAG plus $IP_3$ (black bar) (0.92 ± 0.38 Hz) ($F_{2,19}$ = 4.691, $P$ = 0.0221, standard ANOVA; $P$ < 0.05 Dunnett multiple comparisons test).

plus $IP_3$ significantly increased the firing frequency of the burst (Fig. 6, inset), but did not alter the amplitude of the depolarization ($F_{2,19} = 0.3972$, $P = 0.6776$, standard ANOVA), duration ($F_{2,19} = 0.6123$, $P = 0.5525$, standard ANOVA) or latency ($F_{2,19} = 1.901$, $P = 0.1768$, standard ANOVA).

## Direct activation of PKC results in a current similar to that evoked by $H_2O_2$

Up to this point, we have considered DAG (i.e. OAG) and $IP_3$ as being independent of other downstream effectors. Nevertheless, since PKC-mediated activation of NOX stimulates $H_2O_2$ production in bag cell neurons (Munnamalai *et al.* 2014), we investigated whether PKC activation can evoke a response similar to the $H_2O_2$-induced current. This was accomplished by treating with phorbol ester to trigger PKC (Castagna et al. 1982; DeRiemer *et al.* 1985; Sossin *et al.* 1993), which should liberate $H_2O_2$ and gate the channel. Cultured neurons were voltage-clamped at −30 mV and dialysed with $Cs^+$-Asp-based intracellular saline, then exposed to either the PKC activator phorbol 12-myristate 13-acetate (PMA; Castagna *et al.* 1982) or a control molecule, 4-$\alpha$-phorbol. Bath-application of 100 nM 4-$\alpha$-phorbol elicited negligible inward current of ∼−10 pA ($n = 6$) (Fig. 7*A*, top, and *B*); however, introducing 100 nM PMA evoked an inward current of ∼−120 pA ($n = 5$) (Fig. 7*A*, bottom, and *B*), similar to a typical $H_2O_2$-induced current. Our prior work showed that $H_2O_2$ gates a non-selective cation channel with a reversal potential of ∼+30 mV (Chauhan & Magoski, 2019). To determine the reversal potential of the PMA-induced current, a 5-s ramp from −60 to +60 mV was delivered from a holding potential of −30 mV (Fig. 7*C*, inset). The ramp was given twice, namely, right before PMA application and again at the peak of the PMA response. A difference current was then calculated by subtracting the first ramp-induced current from the second ramp-induced current. Like the $H_2O_2$-induced current (Chauhan & Magoski, 2019), the difference current in PMA was non-linear (U-shaped), inward, voltage-dependent and reversed at ∼+30 mV ($n = 5$) (Fig. 7*C* and *D*). Employing 4-$\alpha$-phorbol as control yielded a difference current with a reversal potential of ∼−40 mV that was mainly outward ($n = 9$) (Fig. 7*C* and *D*). In some cases, the outward current in 4-$\alpha$-phorbol showed some inward rectification above 0 mV, with an apparent decrease at positive potentials. This may be due to incomplete $K^+$ channel block by $Cs^+$ in the intracellular saline, or voltage-dependent relief of that block (Colmers *et al.* 1982), or a residual outward $H^+$ current (Johnson & Byerly, 1993). The reversal potential in PMA was significantly different from that in 4-$\alpha$-phorbol (Fig. 7*D*).

## PKC activation boosts $H_2O_2$-induced action potential firing

Given that PKC is triggered 2–5 min from afterdischarge onset (Conn *et al.* 1989; Wayne *et al.* 1999), we studied the effect of PKC activation in conjunction with $H_2O_2$ on bag cell neuron activity. Cultured neurons were current-clamped with $K^+$-Asp-based intracellular saline and, from a resting potential of −40 mV, 100 nM 4-$\alpha$-phorbol was introduced to the bath, followed by

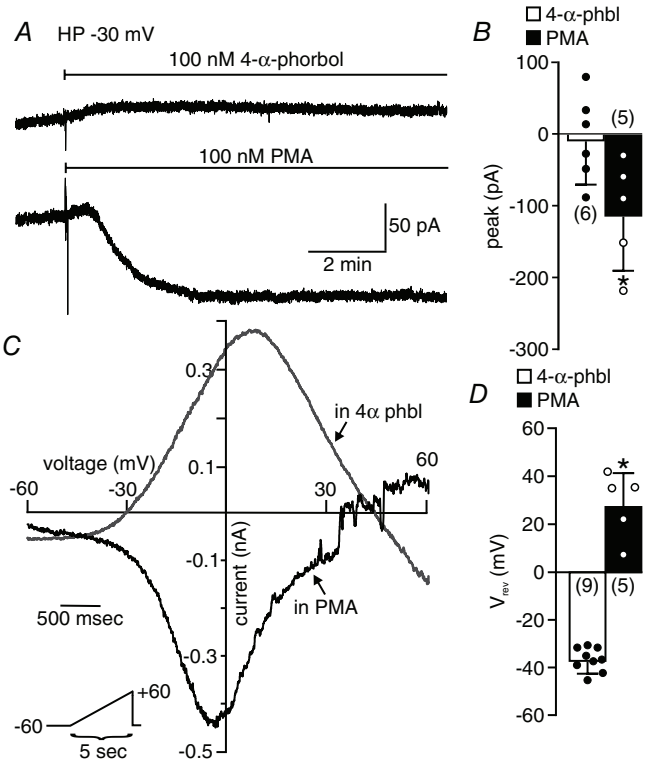


**Figure 7. PMA causes an inward current consistent with the $H_2O_2$-induced current**
*A*, cultured bag cell neurons were voltage-clamped at −30 mV. Bath-application (at bar) of 100 nM of the inactive 4-$\alpha$-phorbol produced a small, outward current (top; $I_{hold} = -127.6$ pA), while in a different neuron, delivery of 100 nM PMA resulted in a noticeable inward current (bottom; $I_{hold} = -81.6$ pA). Scale bars apply to both traces. *B*, group data demonstrating that, in comparison to 4-$\alpha$-phorbol (−9.1 ± 60.7 pA), the current induced by PMA (−114.4 ± 75.8 pA) was significantly larger ($t_{(9)} = 2.565$; $P = 0.0304$; unpaired Student's *t*-test). *C*, difference currents obtained by subtracting the response to a 5 s, −60 to +60 mV voltage ramp (bottom inset), taken immediately before 100 nM 4-$\alpha$-phorbol (grey) or PMA (black) application, from that taken at peak of the response. The current in the presence of 4-$\alpha$-phorbol reversed at ∼−30 mV and was largely outward over the voltage range, with subsequent inward rectification beginning at ∼+10 mV. In PMA, the voltage dependence resulted in a U-shaped inward current with a reversal of ∼+35 mV. *D*, summary data illustrating a significant difference in the reversal potential of 4-$\alpha$-phorbol (−37.7 ± 5.0 mV) *vs.* PMA (27.0 ± 13.8 mV) ($t_{(13)} = 10.618$; $P < 0.0001$, unpaired Student's *t*-test).

application of 1 mM $H_2O_2$ ∼15 min later. This regimen evoked a burst of action potentials (Fig. 8*A*, top) comparable to what we had reported earlier (Chauhan & Magoski, 2019). Here, these bursts had an onset latency of ∼4 min ($n = 5$) and a duration of ∼7 min ($n = 6$) (Fig. 8*B*). When 100 nM PMA and $H_2O_2$ were delivered in a similar fashion, they also produced spiking (Fig. 8*A*, bottom); however, the duration of firing was significantly increased to ∼13 min ($n = 7$), while the onset latency was significantly decreased to ∼2 min ($n = 7$) (Fig. 8*B*).

## Acetylcholine-evoked bursts in bag cell neuron clusters are diminished by a NOX inhibitor

Previous work suggests PKC activation stimulates $H_2O_2$ production (Munnamalai *et al.* 2014), which we assert would gate the cation channel and cause bursting (Chauhan & Magoski, 2019). However, these data are from cultured bag cell neurons; as such, we attempted to obtain evidence that endogenous $H_2O_2$ contributes to bursting in the bag cell neuron network. Specifically, whole bag cell neuron clusters were isolated and sharp-electrode current-clamp recordings made from individual neurons within the cluster (see Methods, 'Animals, ethical approval and cell culture' and 'Sharp-electrode recording from bag cell neurons in isolated clusters' for details).

To elicit afterdisharge-like responses, 1 mM acetylcholine was pressure-ejected onto one side of the cluster while recording from a neuron on the other side. We opted to isolate the clusters because our earlier work showed that acetylcholine was more effective in this configuration (White & Magoski 2012; White *et al.* 2018), likely due to high levels of acetylcholinesterase within the surrounding connective tissue of clusters in the intact ganglion (Giller & Schwartz, 1971). Moreover, this allowed us to assign one cluster from a given animal to the DMSO-pretreated control group, while the second cluster was placed in an experimental group pretreated for ∼15 min with 5 $\mu$M of the pan-NOX inhibitor 3-benzyl-7-(2-benzoxazolyl)thio-1,2,3-triazolo[4,5-d] pyrimidine (VAS2870; ten Freyhaus *et al.* 2006), which has been used previously in bag cell neurons (Munnamalai *et al.* 2014). Prior to delivering acetylcholine, all neurons were tested for excitability using a brief train of depolarizing current pulses; action potentials could be readily evoked in both DMSO- ($n = 4$) and VAS2870-treated ($n = 4$) clusters (Fig. 9*A*). Yet, while neurons from control clusters consistently responded to acetylcholine with an ∼30 mV depolarization and a 0.6 ± 0.4 Hz burst of spikes lasting 2.3 ± 0.6 min (Fig. 9*B*, top), those in the NOX inhibitor only depolarized by ∼13 mV and never fired action potentials (Fig. 9*B*, bottom). Furthermore, during the depolarization in VAS2870-treated clusters there was no evidence of electro-

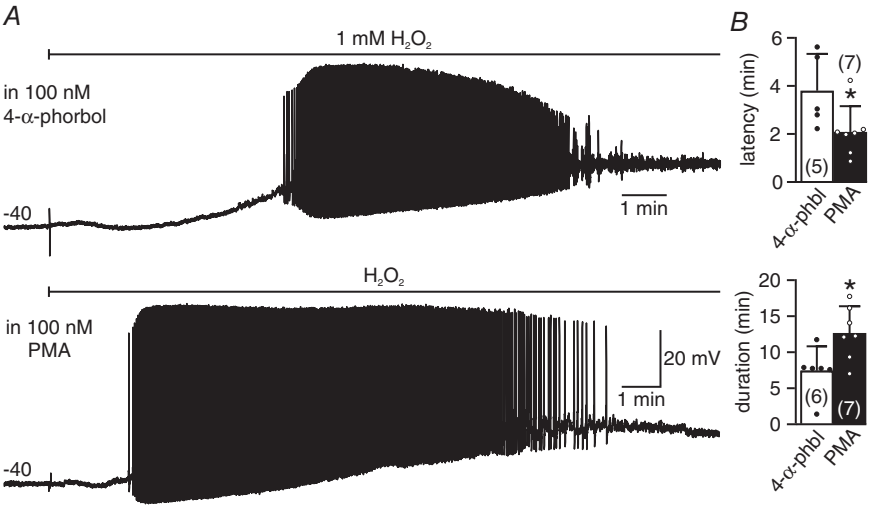


**Figure 8. PMA increases the duration and decreases the latency of action potential firing**
*A*, current-clamp recording from separate cultured bag cell neurons initially set to −40 mV with bias current. Bath-application (at bar) of 1 mM $H_2O_2$ in the presence of 100 nM 4-$\alpha$-phorbol depolarized the membrane potential and caused persistent action potential firing (top). Exposure to 1 mM $H_2O_2$ in the presence of 100 nM PMA resulted in a more rapid onset and longer lasting burst of action potentials (bottom). Ordinate applies to both traces. *B*, average data illustrating that in comparison to 4-$\alpha$-phorbol (3.8 ± 1.5 min), PMA (2.1 ± 1.1 min) significantly decreased the onset latency (top) ($U_{5,7} = 3.0$; $P = 0.0177$; Mann–Whitney *U*-test). In addition, the duration (bottom) of the $H_2O_2$-evoked burst was significantly increased with PMA (12.6 ± 3.8 min) *vs.* 4-$\alpha$-phorbol (7.4 ± 3.4 min) ($U_{6,7} = 6.0$; $P = 0.0350$; Mann–Whitney *U*-test).

tonic potentials, suggesting that other neurons in the cluster were also not reaching threshold. Because electrical coupling within the cluster is extensive and spiking is synchronous (Dargaei et al. 2014, 2015), one neuron can report the activity of the entire cluster. The initial resting membrane potential of the neurons before acetylcholine was not significantly different between groups (Fig. 9*C*, top), although the extent of the depolarization to acetylcholine was significantly different (Fig. 9*C*, bottom).

## Discussion

Short-term synaptic input to the bag cell neurons is converted into a long-term afterdischarge that outlasts the stimulus many times over (Kupfermann & Kandel, 1970). In the nervous system, fast synaptic transmission of acetylcholine onto bag cell neurons opens ionotropic, nicotinic-type receptors to commence depolarization and action potential firing (White & Magoski, 2012) (Fig. 10*A* and *B*). Through a currently unknown mechanism (non-muscarinic), PLC is then activated to liberate DAG plus $IP_3$ (Fink *et al.* 1988; Conn *et al.* 1989); in turn, DAG triggers PKC, which stimulates NOX to produce $H_2O_2$ (Wayne *et al.* 1999; Munnamalai *et al.* 2014) (Fig. 10*C*). Spiking is maintained through cation channels gated by both $H_2O_2$ and DAG plus $IP_3$ (Sturgeon & Magoski, 2016; Chauhan & Magoski, 2019). We now show that DAG and $IP_3$ also directly augment the $H_2O_2$-induced current (Fig. 10*C*); the mechanism may involve direct interaction with the channel, but does not appear to require $Ca^{2+}$ release from intracellular stores. The ultimate consequence of the afterdischarge is secretion of egg-laying hormone, which causes the extrusion of eggs from the ovotestis (Fig. 10*D*).

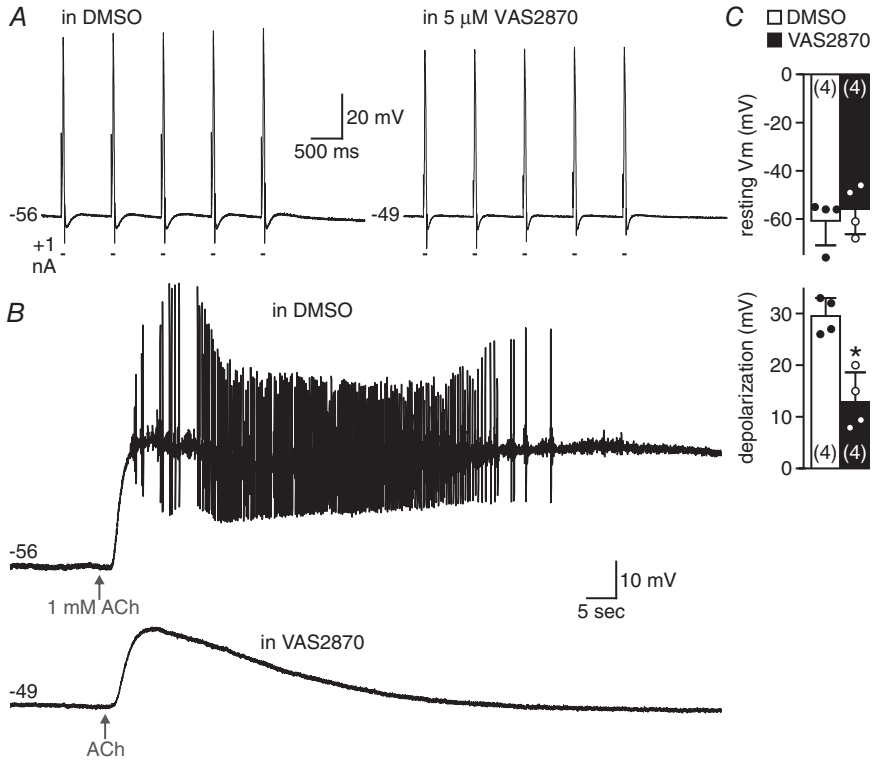


**Figure 9. Blocking NOX attenuates acetylcholine-induced bursting in desheathed bag cell neuron clusters**
*A*, sharp-electrode current-clamp recordings were made from neurons in isolated bag cell neuron clusters treated for ∼15 min with either DMSO or 5 $\mu$M of the pan-NOX inhibitor VAS2870. In either condition, an ∼1 Hz train-stimulus of 1 nA depolarizing current injections readily induced a series of five action potentials. Scale bars apply to both traces. *B*, in the presence of DMSO, a 20 s, 1 mM pressure-ejection (at arrow) of acetylcholine (ACh) to one side of the cluster depolarized and led to a burst in a neuron recorded on the opposite side of the cluster (top). In a separate cluster exposed to VAS2870, acetylcholine caused depolarization of the neuron, but failed to evoke action potentials (bottom). Scale bars apply to both traces. *C*, summary data demonstrating no significant difference in the initial average resting membrane potential ($V_m$) of neurons in clusters treated with DMSO (−60.8 ± 10.2 mV) *vs.* VAS2870 (−56.0 ± 10.3 mV) (top) ($t_{(6)}$ = 0.6562; $P$ = 0.5360; unpaired Student's *t*-test); however, there was a significant reduction in the mean acetylcholine-induced depolarization in DMSO (29.5 ± 3.5 mV) *vs.* VAS2870 (13.1± 5.5 mV) (bottom) ($t_{(6)}$ = 5.011; $P$ = 0.0024; unpaired Student's *t*-test).

Earlier, we showed that exogenous $H_2O_2$ evokes bursting reminiscent of an afterdischarge by gating a voltage-dependent cation current (Chauhan & Magoski, 2019). The $H_2O_2$-induced current has the same biophysics, ion selectivity and pharmacology of a conductance originally characterized by Wilson *et al.* (1996) and studied extensively at the single-channel level (Magoski, 2004; Gardam & Magoski, 2009; Geiger *et al.* 2009; Sturgeon & Magoski, 2018). Given the depolarization associated with the afterdischarge, continuous voltage-gating of this current likely occurs throughout the burst (Wilson *et al.* 1996; Gardam & Magoski, 2009).

Our laboratory found that the activity of single cation channels in excised-patches was potentiated by exogenous OAG/$IP_3$ or activation of endogenous PLC with *m*-3M3FBS (Sturgeon & Magoski, 2018). OAG has been shown to activate the TRPC3/6/7 cation channels (Hofmann et al. 1999; Okada *et al.* 1999; Venkatachalam *et al.* 2003), as well as a TRPC-like conductance in cortical neurons (Tu *et al.* 2009). Here, we link our single-channel findings to the whole-cell level by demonstrating that the $H_2O_2$-induced current is also potentiated by phosphoinositide metabolites. In the presence of OAG, $H_2O_2$ elicits a larger inward current compared to control. Such an outcome may be due to the simultaneous activation of the cation channel by OAG and $H_2O_2$, or the influence of a change in redox enhancing lipid interactions with the channel. This is in line with reports of TRPC3/4 channels sensing redox modification of the channel-lipid membrane environment (Poteser *et al.* 2006; Malczyk *et al.* 2016). TRPC6 channels also appear to be directly activated by $H_2O_2$, and this is sensitized by OAG (Graham *et al.* 2010). Parenthetically, although it is a DAG analogue, it is unlikely that the effects of OAG are mediated by PKC. Both our prior work on bag cell neurons (Sturgeon & Magoski, 2016) and experiments involving TRPC3 and C6 in cell lines (Hofmann *et al.* 1999) find OAG does not activate PKC.

We previously established that delivery of $IP_3$ to excised patches increases the stimulatory effect of OAG on cation channel activity (Sturgeon & Magoski, 2018). Therefore, we perfused $IP_3$ directly into the neuron via the whole-cell pipette and found that $IP_3$ alone modestly increases the $H_2O_2$-induced current, while co-application of OAG plus $IP_3$ markedly enhances the response even further. DAG and $IP_3$ impact several conductances, including connexins and various $K^+$ channels, as well as native and TRP cation

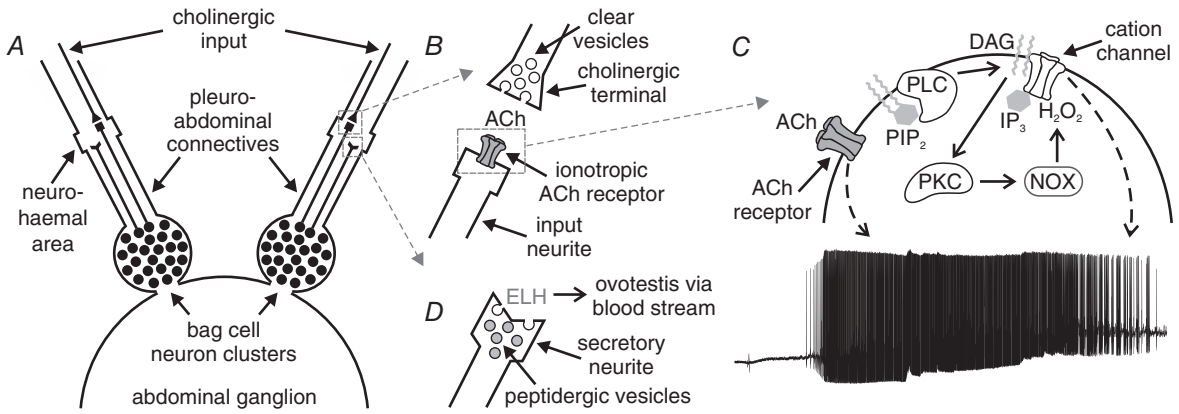


**Figure 10. Potential role for phosphoinositides and $H_2O_2$ in maintaining the afterdischarge**
*A*, schematic representation of the *Aplysia* abdominal ganglion, with bag cell neurons located in two clusters at the rostral end. Cholinergic synaptic input (triangular endings) descends from the central nervous system through the pleuroabdominal connectives to innervate bag cell neurons on input neurites (square endings). Egg-laying hormone is released from secretory neurites (fletched endings) into the circulation at neurohaemal areas in the connectives. *B*, top dashed box from *A* expanded. Acetylcholine (ACh) from cholinergic terminals binds to ionotropic acetylcholine receptors on input neurites. *C*, dashed box from *B* expanded. Gating of the acetylcholine receptor triggers the afterdischarge. Subsequent activation, through a currently unknown mechanism, of phospholipase C (PLC) results in hydrolysis of the membrane lipid phosphatidylinositol 4,5-bisphosphate ($PIP_2$) into inositol trisphosphate ($IP_3$) and diacylglycerol (DAG). Protein kinase C (PKC) is then turned on by DAG, which stimulates nicotinamide adenine dinucleotide phosphate oxidase (NOX) to produce $H_2O_2$. A non-selective, voltage-dependent cation channel is opened by $H_2O_2$, and this is enhanced by binding of both DAG and $IP_3$. Inward current, transiently from the acetylcholine receptor, and then more persistently from the $H_2O_2$-gated channel, provides depolarization to drive spiking during the afterdischarge. *D*, bottom dashed box from *A* expanded. The afterdischarge results in activity-dependent release of egg-laying hormone (ELH) from secretory neurites into the blood stream, which causes egg deposition by acting on muscles encompassing gonadal follicles in the ovotestis. Based on the present work as well as Coggeshall (1970), Arch (1972), Haskins *et al.* (1981), Fink *et al.* (1988), Loechner *et al.* (1990), Wilson et al. (1996), Wayne *et al.* (1999), White & Magoski (2012), Sturgeon & Magoski (2016, 2018) and Chauhan & Magoski (2019).

channels (Estacion *et al*. 2001; Gamper & Shapiro, 2007; van Zeijl *et al*. 2007; Song *et al*. 2015). In particular, Albert & Large (2003) demonstrated similar synergism between OAG and $IP_3$ in activating a TRPC6-like current. For bag cell neurons, we assert that, along with OAG, $IP_3$ is most likely acting directly on the channel, rather than by releasing intracellular $Ca^{2+}$. This is based on the present results that the $IP_3$ receptor blocker heparin did not alter the action of $IP_3$ on the $H_2O_2$-induced current, nor did liberating $Ca^{2+}$ from the endoplasmic reticulum with CPA mimic the effect of $IP_3$. Furthermore, the influence of $IP_3$ on the cation channel can be observed in excised, inside-out patches, where the endoplasmic reticulum is absent (Sturgeon & Magoski, 2018), suggesting $IP_3$ is binding to the channel or an associated protein.

In addition to exogenous phosphoinositide metabolites, we also sought to determine if directly turning on PLC via *m*-3M3FBS is sufficient to release adequate amounts of DAG and/or $IP_3$ to modulate the $H_2O_2$-induced current. This PLC activator has been previously shown to both increase neurite outgrowth in bag cell neurons (Zhang *et al*. 2012) and augment the cation channel in cell-free patches (Sturgeon & Magoski, 2018). The latter suggests PLC is in some capacity physically associated with the channel. Here, we find that prior exposure to *m*-3M3FBS significantly enhances the $H_2O_2$-induced current. In comparison to OAG alone, the use of the PLC activator leads to a larger $H_2O_2$-induced current. The direct production of DAG via *m*-3M3FBS *vs*. just exogenously applying OAG could account for this difference. Possibly, activating PLC, which is membrane-bound, might alter the complex between the enzyme and the channel, thereby enhancing the ability of $H_2O_2$ to gate the current. Alternatively, the more effective action of *m*-3M3FBS may arise from PLC activation producing both DAG and $IP_3$, compared to OAG (in place of DAG) application alone. Overall, the activation of PLC with *m*-3M3FBS resulted in a similar outcome to OAG plus $IP_3$.

Because PLC activation occurs at the beginning of the slow phase (Fink *et al*. 1988) it would result in OAG and $IP_3$ being available to interact with the $H_2O_2$ liberated by PKC. The exact mechanism of PLC activation during the afterdischarge is unknown, but voltage-gated $Ca^{2+}$-influx or autoreceptors may trigger the enzyme (DeReimer et al. 1985; Loechner & Kaczmarek, 1994; Thore *et al*. 2004; Murata *et al*. 2005). Synergistic modulation by lipid metabolites could maintain the cation current to drive action potentials during the afterdischarge. For bag cell neurons exposed to OAG plus $IP_3$, delivery of $H_2O_2$ leads to spiking reminiscent of the frequency during the slow phase of the afterdischarge, that is, ∼1 Hz. Similar to what is seen at the single-channel level (Sturgeon & Magoski, 2018), OAG plus $IP_3$ may prime the cation channel to other gating factors, like voltage, and boost the response to $H_2O_2$. Lipid-induced modulation of the $H_2O_2$-induced current may be necessary to achieve the requisite firing frequency that the $H_2O_2$ alone-induced current cannot produce. Interestingly, the burst response to $H_2O_2$ in the presence of just OAG is essentially the same as with OAG plus $IP_3$; thus, the synergy seen for membrane current, where $H_2O_2$ in OAG plus $IP_3$ is the strongest, does not translate to a faster frequency. Potentially, voltage-dependent effects on the spike-generation mechanism ($Na^+$ or $Ca^{2+}$ current inactivation; more $K^+$ currents) may dampen the membrane potential response to a greater $H_2O_2$-induced current in the presence of OAG plus $IP_3$.

$H_2O_2$ has emerged as an ion channel modulator due to its ability to oxidize lipids or proteins (Gutteridge & Halliwell, 1992; Halliwell, 1992; Kamsler & Segal, 2004; Kishida & Klann, 2007). For example, TRPM2 is expressed in neurons and microglia, and can be gated by $H_2O_2$ (Perraud *et al*. 2001; Sano *et al*. 2001; Kraft *et al*. 2004; Tong *et al*. 2006). For substantia nigra GABAergic neurons, $H_2O_2$ enhances spontaneous firing through cation channel activation, as well as by interacting with NMDA-receptor-dependent bursting (Lee *et al*. 2013). Since PKC likely stimulates $H_2O_2$ production through phosphorylation of the NOX cytosolic regulatory subunit, $p47^{phox}$ (Fontayne *et al*. 2002), it may be acting in bag cell neurons concordant with afterdischarge generation. Consistent with this, preventing $H_2O_2$ generation with the NOX inhibitor VAS2870 lessens the depolarization and eliminates the bursting elicited by acetylcholine in isolated clusters. Hence, NOX activation (and presumably $H_2O_2$ production) appears critical to prolonging burst firing. As for PKC itself, activation by the phorbol ester PMA brings about a more rapid onset and longer duration of the $H_2O_2$-induced burst. Possibly, PMA-mediated PKC activation leads to $H_2O_2$ generation and cation channel activation. Under voltage-clamp, PMA evokes an inward current that is voltage-dependent and presents a U-shaped current–voltage curve with a reversal of ∼+30 mV, reflecting the $Ca^{2+}$ permeability of this conductance. This curve is essentially the same as that for the cation current originally characterized by Wilson *et al*. (1996) and the $H_2O_2$-induced current (Chauhan & Magoski, 2019). Thus, both intracellularly produced and exogenously applied $H_2O_2$ may cause the decrease in latency and an increase in spike duration.

The PLC pathway appears to be imperative for maintaining the afterdischarge. By activating PKC (DeRiemer *et al*. 1985; Wayne *et al*. 1999), DAG not only leads to $H_2O_2$ synthesis (Munnamalai *et al*. 2014), but also enhances $Ca^{2+}$ channels and peptide release (Loechner *et al*. 1992; Groten & Magoski, 2015), as well as gap junctions (Beekharry *et al*. 2018). We now conclude that DAG and $IP_3$ also influence the $H_2O_2$-induced cation current to promote the action potential firing necessary for hormone secretion and reproduction.

## References


Albert AP & Large WA (2003). Synergism between inositol phosphates and diacylglycerol on native TRPC6-like channels in rabbit portal vein myocytes. *J Physiol* **552**, 789–795.

Arch S (1972). Polypeptide secretion from the isolated parietovisceral ganglion of *Aplysia californica*. *J Gen Physiol* **59**, 47–59.

Babior BM, Kipnes RS & Curnutte JT (1973). Biological defense mechanisms: the production by leukocytes of superoxide, a potential bactericidal agent. *J Clin Invest* **52**, 741–744.

Bae YS, Lee TG, Park JC, Hur JH, Kim Y, Heo K, Kwak JY, Suh PG & Ryu SH (2003). Identification of a compound that directly stimulates phospholipase C activity. *Mol Pharmacol* **63**, 1043–1050.

Bedard K & Krause KH (2007). The NOX family of ROS-generating NADPH oxidases: physiology and pathophysiology. *Physiol Rev* **87**, 245–313.

Beekharry CC, Gu Y & Magoski NS (2018). Protein kinase C enhances electrical synaptic transmission by acting on junctional and postsynaptic $Ca^{2+}$ currents. *J Neurosci* **38**, 2796–2808.

Berridge MJ & Irvine RF (1989). Inositol phosphates and cell signalling. *Nature* **341**, 197–205.

Boveris A & Chance B (1973). The mitochondrial generation of hydrogen peroxide. General properties and effect of hyperbaric oxygen. *Biochem J* **134**, 707–716.

Brookes PS, Yoon Y, Robotham JL, Anders MW & Sheu SS (2004). Calcium, ATP, and ROS: a mitochondrial love-hate triangle. *Am J Physiol Cell Physiol* **287**, C817–C833.

Bychkov R, Pieper K, Ried C, Milosheva M, Bychkov E, Luft FC & Haller H (1999). Hydrogen peroxide, potassium currents, and membrane potential in human endothelial cells. *Circulation* **99**, 1719–1725.

Carlson RO & Levitan IB (1990). Regulation of intracellular free arachidonic acid in *Aplysia* nervous system. *J Membr Biol* **116**, 249–260.

Castagna M, Takai Y, Kaibuchi K, Sano K, Kikkawa U & Nishizuka Y (1982). Direct activation of calcium-activated, phospholipid-dependent protein kinase by tumor-promoting phorbol esters. *J Biol Chem* **257**, 7847–7851.

Chang DJ, Lim CS, Lee SH & Kaang BK (2003). Hydrogen peroxide modulates $K^+$ ion currents in cultured *Aplysia* sensory neurons. *Brain Res* **970**, 159–168.

Chauhan AK & Magoski NS (2019). Hydrogen peroxide gates a voltage-dependent cation channel in *Aplysia* neuroendocrine cells. *J Neurosci* **39**, 9900–9913.

Coggeshall RE (1970). A cytologic analysis of the bag cell control of egg laying in *Aplysia*. *J Morphol* **132**, 461–485.

Colmers WF, Lewis DV Jr & Wilson WA (1982) $Cs^+$ loading reveals $Na^+$-dependent persistent inward current and negative slope resistance region in *Aplysia* giant neurons. *J Neurophysiol* **48**, 1191–1200.

Conn PJ & Kaczmarek LK (1989). The bag cell neurons of *Aplysia*: a model for the study of the molecular mechanisms involved in the control of prolonged animal behaviors. *Mol Neurobiol* **3**, 237–273.

Conn PJ, Strong JA & Kaczmarek LK (1989). Inhibitors of protein kinase C prevent enhancement of calcium current and action potentials in peptidergic neurons of *Aplysia*. *J Neurosci* **9**, 480–487.

Dargaei Z, Colmers PLW, Hodgson HM & Magoski NS (2014). Electrical coupling between *Aplysia* bag cell neurons: characterization and role in synchronous firing. *J Neurophysiol* **112**, 2680–2696.

Dargaei Z, Standage D, Groten CJ, Blohm G & Magoski NS (2015). $Ca^{2+}$-induced uncoupling of *Aplysia* bag cell neurons. *J Neurophysiol* **113**, 808–821.

DeRiemer SA, Greengard P & Kaczmarek LK (1985). Calcium/phosphatidylserine/diacylglycerol-dependent protein phosphorylation in the *Aplysia* nervous system. *J Neurosci* **5**, 2672–2676.

Dong HW, Hayar A, Callaway J, Yang XH, Nai Q & Ennis M (2009). Group I mGluR activation enhances $Ca^{2+}$-dependent nonselective cation currents and rhythmic bursting in main olfactory bulb external tufted cells. *J Neurosci* **29**, 11943–11953.

Estacion M, Sinkins WG & Schilling WP (2001). Regulation of *Drosophila* transient receptor potential-like (TrpL) channels by phospholipase C-dependent mechanisms. *J Physiol* **530**, 1–19.

Fink LA, Connor JA & Kaczmarek LK (1988). Inositol trisphosphate releases intracellularly stored calcium and modulates ion channels in molluscan neurons. *J Neurosci* **8**, 2544–2555.

Fisher TE, Levy S & Kaczmarek LK (1994). Transient changes in intracellular calcium associated with a prolonged increase in excitability in neurons of *Aplysia californica*. *J Neurophysiol* **71**, 1254–1257.

Flockerzi V (2004). Non-selective cation channels. In *Encyclopedia of Molecular Pharmacology*, ed. Offermanns S & Rosenthal W. Springer, Berlin, Heidelberg, https://doi.org/10.1007/3-540-29832-0_1145

Fontayne A, Dang PM, Gougerot-Pocidalo MA & El-Benna J (2002). Phosphorylation of $p47^{phox}$ sites by PKC $\alpha$, beta II, $\delta$, and $\zeta$: effect on binding to p22phox and on NADPH oxidase activation. *Biochemistry* **41**, 7743–7750.

Gamper N & Shapiro M (2007). Regulation of ion transport proteins by membrane phosphoinositides. *Nat Rev Neurosci* **8**, 921–934.

Gardam KE & Magoski NS (2009). Regulation of cation channel voltage- and $Ca^{2+}$-dependence by multiple modulators. *J Neurophysiol* **102**, 259–271.

Geiger JE, Hickey CM & Magoski NS (2009). $Ca^{2+}$ entry through a nonselective cation channel in *Aplysia* bag cell neurons. *Neuroscience* **162**, 1023–1038.

Geiger JE & Magoski NS (2008). $Ca^{2+}$-induced $Ca^{2+}$-release in *Aplysia* bag cell neurons requires interaction between mitochondrial and endoplasmic reticulum stores. *J Neurophysiol* **100**, 24–37.

Ghamari-Langroudi M & Borque WC (2002). Flufenamic acid blocks depolarization afterpotentials and phasic firing in rat supraoptic neurones. *J Physiol* **545**, 537–542.

Ghosh TK, Eis PS, Mullaney JM, Ebert CL & Gill DL (1988). Competitive, reversible, and potent antagonism of inositol 1,4,5-triphosphate-activated calcium release by heparin. *J Biol Chem* **263**, 11075–11079.

Giller E & Schwartz JH (1971). Acetylcholinesterase in identified neurons of abdominal ganglion of *Aplysia californica*. *J Neurophysiol* **34**, 108–115.

Graham S, Ding M, Ding Y, Sours-Brothers S, Luchowski R, Gryczynski Z, Yorio T, Ma H & Ma R (2010). Canonical transient receptor potential 6 (TRPC6), a redox-regulated cation channel. *J Biol Chem* **285**, 23466–23476.

Groten CJ & Magoski NS (2015). PKC enhances the capacity for secretion by rapidly recruiting covert voltage-gated $Ca^{2+}$ channels to the membrane. *J Neurosci* **35**, 2747–2765.

Groten CJ, Rebane JT, Blohm G & Magoski NS (2013). Separate $Ca^{2+}$ sources are buffered by distinct $Ca^{2+}$ handling systems in *Aplysia* neuroendocrine cells. *J Neurosci* **33**, 6476–6491.

Gutteridge JM & Halliwell B (1992). Comments on review of free radical in biology and medicine, second edition. *Free Radic Biol Med* **12**, 93–94.

Halliwell B (1992). Reactive oxygen species and the central nervous system. *J Neurochem* **59**, 1609–1623.

Hamill OP, Marty A, Neher E, Sakmann B & Sigworth FJ (1981). Improved patch-clamp techniques for high-resolution current recording from cells and cell-free membrane patches. *Pflugers Arch* **391**, 85–100.

Hansen SB (2015). Lipid agonism: the $PIP_2$ paradigm of ligand-gated ion channels. *Biochim Biophys Acta* **1851**, 620–628.

Hardie RC (2007). TRP channels and lipids: from *Drosophila* to mammalian physiology. *J Physiol* **578**, 9–24.

Haskins JT, Price CH & Blankenship JE (1981). A light and electron microscopic investigation of the neurosecretory bag cells of *Aplysia*. *J Neurocytol* **10**, 729–747.

Helliwell RM & Large WA (1997). $\alpha_1$-Adrenoceptor activation of a non-selective cation current in rabbit portal vein by 1,2-diacyl-*sn*-glycerol. *J Physiol* **499**, 417–428.

Hickey CM, Geiger KE, Groten CJ & Magoski NS (2010). Mitochondrial $Ca^{2+}$ activates a cation current in *Aplysia* bag cell neurons. *J Neurophysiol* **103**, 1543–1556.

Hill K, Tigue NJ, Kelsell RE, Benham CD, McNulty S, Schaefer M & Randall AD (2006). Characterisation of recombinant rat TRPM2 and a TRPM2-like conductance in cultured rat striatal neurones. *Neuropharmacology* **50**, 89–97.

Hille B, Dickson EJ, Kruse M, Vivas O & Suh BC (2015). Phosphoinositides regulate ion channels. *Biochim Biophys Acta* **1851**, 844–856.

Hofmann T, Obukhov AG, Schaefer M, Harteneck C, Gudermann T & Schultz G (1999). Direct activation of human TRPC6 and TRPC3 channels by diacylglycerol. *Nature* **397**, 259–263.

Johnson BD & Byerly L (1993). A cytoskeletal mechanism for $Ca^{2+}$ channel metabolic dependence and inactivation by intracellular $Ca^{2+}$. *Neuron* **10**, 797–804.

Jonas EA, Knox RJ, Smith TCM, Wayne NL, Connor JA & Kaczmarek LK (1997). Regulation by insulin of a unique neuronal $Ca^{2+}$ pool and neuropeptide secretion. *Nature* **385**, 343–346.

Kachoei BA, Knox RJ, Uthuza D, Levy S, Kaczmarek LK & Magoski NS (2006). A store-operated $Ca^{2+}$ influx pathway in the bag cell neurons of *Aplysia*. *J Neurophysiol* **96**, 2688–2698.

Kaczmarek LK, Jennings KR & Strumwasser F (1982). An early sodium and a late calcium phase in the afterdischarge of peptide-secreting neurons of *Aplysia*. *Brain Res* **238**, 105–115.

Kamsler A & Segal M (2004). Hydrogen peroxide as a diffusible signal molecule in synaptic plasticity. *Mol Neurobiol* **29**, 167–178.

Kishida KT & Klann E (2007). Sources and targets of reactive oxygen species in synaptic plasticity and memory. *Antioxid Redox Signal* **9**, 233–244.

Knauer B, Jochems A, Valero-Aracama MJ & Yoshida M (2013). Long-lasting intrinsic persistent firing in rat CA1 pyramidal cells: a possible mechanism for active maintenance of memory. *Hippocampus* **23**, 820–831.

Kononenko NI, Medin I & Dudek FE (2004). Persistent subthreshold voltage-dependent cation single channels in suprachiasmatic nucleus neurons. *Neuroscience* **129**, 85–92.

Kraft R, Grimm C, Grosse K, Hoffmann A, Sauerbruch S, Kettenmann H, Schultz G & Harteneck C (2004). Hydrogen peroxide and ADP-ribose induce TRPM2-mediated calcium influx and cation currents in microglia. *Am J Physiol* **286**, C129–C137.

Kupfermann I (1967). Stimulation of egg laying: possible neuroendocrine function of bag cell neurons of abdominal ganglion of *Aplysia californica*. *Nature* **216**, 814–815.

Kupfermann I & Kandel ER (1970). Electrophysiological properties and functional interconnections of two symmetrical neurosecretory clusters (bag cells) in abdominal ganglion of *Aplysia*. *J Neurophysiol* **33**, 865–876.

Lee CR, Witkovsky P & Rice ME (2011). Regulation of substantia nigra pars reticulata GABAergic neuron activity by $H_2O_2$ via flufenamic acid-sensitive channels and $K^+$-ATP channels. *Front Syst Neurosci* **5**, 14.

Lee CR, Machold RP, Witkovsky P & Rice ME (2013). TRPM2 channels are required for NMDA-induced burst firing and contribute to $H_2O_2$-dependent modulation in substantia nigra pars reticulate GABAergic neurons. *J Neurosci* **33**, 1157–1168.

Loechner KJ, Azhderian EM, Dreyer R & Kaczmarek LK (1990). Progressive potentiation of peptide release during a neuronal discharge. *J Neurophysiol* **63**, 738–744.

Loechner KJ & Kaczmarek LK (1994). Autoactive peptides act at three distinct receptors to depolarize the bag cell neurons of *Aplysia*. *J Neurophysiol* **71**, 195–203.

Loechner KJ, Knox RJ, Connor JA & Kaczmarek LK (1992). Hyperosmotic media inhibit voltage dependent calcium influx and peptide release in *Aplysia* neurons. *J Membr Biol* **128**, 41–52.

Lupinsky DA & Magoski NS (2006). $Ca^{2+}$-dependent regulation of a nonselective cation channel from *Aplysia* bag cell neurones. *J Physiol* **575**, 491–506.

Magoski NS (2004). Regulation of an *Aplysia* bag cell neuron cation channel by closely associated protein kinase A and a protein phosphatase. *J Neurosci* **24**, 6833–6841.

Magoski NS & Kaczmarek LK (2004). Protein kinases and neuronal excitability. In *Encyclopedia of Neuroscience*, 3rd edn, ed. Adelman G & Smith BH, CD-ROM. Elsevier.

Magoski NS, Knox RJ & Kaczmarek LK (2000). Activation of a $Ca^{2+}$-permeable cation channel produces a prolonged attenuation of intracellular $Ca^{2+}$ release in *Aplysia* bag cell neurones. *J Physiol* **522**, 271–283.

Magoski NS, Wilson GF & Kaczmarek LK (2002). Protein kinase modulation of a neuronal cation channel requires protein-protein interactions mediated by an Src homology 3 domain. *J Neurosci* **22**, 1–9.

Malczyk M, Veith C, Schermuly RT, Gudermann T, Dietrich A, Sommer N & Weissmann N (2016). NADPH oxidases-do they play a role in TRPC regulation under hypoxia? *Pflugers Arch* **468**, 23–41.

Michel S & Wayne NL (2002). Neurohormone secretion persists after post-afterdischarge membrane depolarization and cytosolic calcium elevation in peptidergic neurons in intact nervous tissue. *J Neurosci* **22**, 9063–9069.

Munnamalai V, Weaver CJ, Weisheit CE, Venkatraman P, Agim ZS, Quinn MT & Suter DM (2014). Bidirectional interactions between NOX2-type NADPH oxidase and the F-actin cytoskeleton in neuronal growth cones. *J Neurochem* **130**, 526–540.

Murata Y, Iwasaki H, Sasaki M, Inaba K & Okamura Y (2005). Phosphoinositide phosphatase activity coupled to an intrinsic voltage sensor. *Nature* **435**, 1239–1243.

Ohashi M, Hirano T, Watanabe K, Katsumi K, Ohashi N, Baba H, Endo N & Kohno T (2016). Hydrogen peroxide modulates synaptic transmission in ventral horn neurons of the rat spinal cord. *J Physiol* **594**, 115–134.

Okada T, Inoue R, Yamazaki K, Maeda A, Kurosaki T, Yamakuni T, Tanaka I, Shimizu S, Ikenaka K, Imoto K & Mori Y (1999). Molecular and functional characterization of a novel mouse transient receptor potential protein homologue TRP7. $Ca^{2+}$-permeable cation channel that is constitutively activated and enhanced by stimulation of G protein-coupled receptor. *J Biol Chem* **274**, 27359–27370.

Olah ME, Jackson MF, Li H, Perez Y, Sun HS, Kiyonaka S, Mori Y, Tymianski M & MacDonald JF (2009). $Ca^{2+}$-dependent induction of TRPM2 currents in hippocampal neurons. *J Physiol* **587**, 965–979.

Partridge LD, Muller TH & Swandulla D (1994). Calcium-activated nonselective channels in the nervous system. *Brain Res Brain Res Rev* **19**, 319–325.

Perraud AL, Fleig A, Dunn CA, Bagley LA, Launay P, Schmitz C, Stokes AJ, Zhu Q, Bessman MJ, Penner R, Kinet JP & Scharenberg AM (2001). ADP-ribose gating of the calcium-permeable LTRPC2 channel revealed by nudix motif homology. *Nature* **411**, 595–599.

Pinsker HM & Dudek FE (1977). Bag cell control of egg laying in freely behaving *Aplysia*. *Science* **197**, 490–493.

Piomelli D, Shapiro E, Feinmark SJ & Schwartz JH (1987). Metabolites of arachidonic acid in the nervous system of *Aplysia*: possible mediators of synaptic modulation. *J Neurosci* **7**, 3675–3686.

Poteser M, Graziani A, Rosker C, Eder P, Derler I, Kahr H, Zhu MX, Romanin C & Groschner K (2006). TRPC3 and TRPC4 associate to form a redox-sensitive cation channel: evidence for expression of native TRPC3-TRPC4 heteromeric channels in endothelial cells. *J Biol Chem* **281**, 13588–13595.

Royer-Pokora B, Kunkel LM, Monaco AP, Goff SC, Newburger PE, Baehner RL, Cole FS, Curnutte JT & Orkin SH (1986). Cloning the gene for an inherited human disorder—chronic granulomatous disease—on the basis of its chromosomal location. *Nature* **322**, 32–38.

Sano Y, Inamura K, Miyake A, Mochizuki S, Yokoi H, Matsushime H & Furuichi K (2001). Immunocyte $Ca^{2+}$ influx system mediated by LTRPC2. *Science* **293**, 1327–1330.

Seidler NW, Jona I, Vegh M & Martonosi A (1989). Cyclopiazonic acid is a specific inhibitor of the $Ca^{2+}$-ATPase of sarcoplasmic reticulum. *J Biol Chem* **264**, 17816–17823.

Shalinsky MH, Magistretti J, Ma L & Alonso AA (2002). Muscarinic activation of a cation current and associated current noise in entorhinal-cortex layer-II neurons. *J Neurophysiol* **88**, 1197–1211.

Sidiropoulou K, Lu FM, Fowler MA, Xiao R, Phillips C, Ozkan ED, Zhu MX, White FJ & Cooper DC (2009). Dopamine modulates an mGluR5-mediated depolarization underlying prefrontal persistent activity. *Nat Neurosci* **12**, 190–199.

Siemen D & Hescheler J (eds) (1993). Nonselective Cation Channels: Pharmacology, Physiology and Biophysics. Birkhäuser, Basel.

Song T, Hao Q, Zheng YM, Liu QH & Wang YX (2015). Inositol 1,4,5-trisphosphate activates TRPC3 channels to cause extracellular $Ca^{2+}$ influx in airway smooth muscle cells. *Am J Physiol Lung Cell Mol Physiol* **309**, L1455–L1466.

Sossin WS, Diaz-Arrastia R & Schwartz JH (1993). Characterization of two isoforms of protein kinase C in the nervous system of *Aplysia californica*. *J Biol Chem* **268**, 5763–5768.

Streb H, Irvine RF, Berridge MJ & Schulz I (1983). Release of $Ca^{2+}$ from a nonmitochondrial intracellular store in pancreatic acinar cells by inositol-1,4,5-trisphosphate. *Nature* **306**, 67–69.

Sturgeon RM & Magoski NS (2016). Diacylglycerol-mediated regulation of *Aplysia* bag cell neuron excitability requires protein kinase C. *J Physiol* **594**, 5573–5592.

Sturgeon RM & Magoski NS (2018). A closely-associated phospholipase C regulates cation channel function through phosphoinositide hydrolysis. *J Neurosci* **38**, 7622–7634.

Svobodova B & Groschner K (2016). Mechanisms of lipid regulation and lipid gating in TRPC channels. *Cell Calcium* **59**, 271–279.

Takai Y, Kishimoto A, Mori T, Kikkawa U & Nishizuka Y (1979). Unsaturated diacylglycerol as a possible messenger for the activation of calcium-activated, phospholipid-dependent protein kinase system. *Biochem Biophys Res Comm* **91**, 1218–1224.

Tam AKH, Gardam KE, Lamb S, Kachoei BA & Magoski NS (2011). Role for protein kinase C in controlling *Aplysia* bag cell neuron excitability. *Neuroscience* **179**, 41–55.

ten Freyhaus H, Huntgeburth M, Wingler K, Schnitker J, Bäumer AT, Vantler M, Bekhite MM, Wartenberg M, Sauer H, Rosenkranz S (2006) Novel Nox inhibitor VAS2870 attenuates PDGF-dependent smooth muscle cell chemotaxis, but not proliferation. *Cardiovasc Res* **71**, 331–341.

Thore S, Dyachok O & Tengholm A (2004). Oscillations of phospholipase C activity triggered by depolarization and $Ca^{2+}$ influx in insulin-secreting cells. *J Biol Chem* **279**, 19396–19400.

Tong Q, Zhang W, Conrad K, Mostoller K, Cheung JY, Peterson BZ & Miller BA (2006). Regulation of the transient receptor potential channel TRPM2 by the $Ca^{2+}$ sensor calmodulin. *J Biol Chem* **281**, 9076–9085.

Tu P, Kunert-Keil C, Lucke S, Brinkmeier H & Bouron A (2009). Diacylglycerol analogues activate second messenger-operated calcium channels exhibiting TRPC-like properties in cortical neurons. *J Neurochem* **108**, 126–138.

van Zeijl L, Ponsioen B, Giepmans BN, Ariaens A, Postma FR, Várnai P, Balla T, Divecha N, Jalink K & Moolenaar WH (2007). Regulation of connexin43 gap junctional communication by phosphatidylinositol 4,5-bisphosphate. *J Cell Biol* **177**, 881–891.

Venkatachalam K, Zheng F & Gill DL (2003). Regulation of canonical transient receptor potential (TRPC) channel function by diacylglycerol and protein kinase C. *J Biol Chem* **278**, 29031–29040.

Wayne NL, Lee W & Kim YJ (1999). Persistent activation of calcium-activated and calcium independent protein kinase C in response to electrical afterdischarge from peptidergic neurons of *Aplysia*. *Brain Res* **834**, 211–213.

Wen PJ, Osborne SL & Meunier FA (2012). Phosphoinositides in neuroexocytosis and neuronal diseases. *Curr Top Microbiol Immunol* **362**, 87–98.

White SH & Magoski NS (2012). Acetylcholine-evoked afterdischarge in *Aplysia* bag cell neurons. *J Neurophysiol* **107**, 2672–2685.

White SH, Sturgeon RM, Gu Y, Nensi A & Magoski NS (2018). Tyrosine phosphorylation determines afterdischarge initiation by regulating an ionotropic cholinergic receptor. *Neuroscience* **372**, 273–288.

Wilson GF, Richardson FC, Fisher TE, Olivera BM & Kaczmarek LK (1996). Identification and characterization of a $Ca^{2+}$-sensitive nonspecific cation channel underlying prolonged repetitive firing in *Aplysia* neurons. *J Neurosci* **16**, 3661–3671.

Yellen G (1982). Single $Ca^{2+}$-activated nonselective cation channels in neuroblastoma. *Nature* **296**, 357–359.

Zhang XF, Hyland C, Van Goor D & Forscher P (2012). Calcineurin-dependent cofilin activation and increased retrograde actin flow drive 5-HT-dependent neurite outgrowth in *Aplysia* bag cell neurons. *Mol Biol Cell* **23**, 4833–4848.

## Additional Information

### Data availability statement

The data that support the findings of this study are available from the corresponding author upon reasonable request.

### Competing interests

The authors declare no competing financial interests.

### Author contributions

A.K.C-P. and N.S.M. conceived and designed the project. A.K.C-P., K.H.L, and N.S.M. conducted the experiments. A.K. C-P. wrote the manuscript. N.S.M. revised the manuscript. All authors have read and approved the final version of this manuscript and agree to be accountable for all aspects of the work in ensuring that questions related to the accuracy or integrity of any part of the work are appropriately investigated and resolved. All persons designated as authors qualify for authorship, and all those who qualify for authorship are listed.

### Acknowledgements

This work was supported by a Canadian Institutes of Health Research operating grant (MOP111211) and project grant (PJT-159794) to N.S.M.

### Keywords

*Aplysia*, diacylglycerol, $H_2O_2$, inositol trisphosphate, mollusc, peptidergic neuron, reproduction

## Supporting information

Additional supporting information can be found online in the Supporting Information section at the end of the HTML view of the article. Supporting information files available:

**Peer Review History**
**Statistical Summary Document**